

Theory of sixth-order wave aberrations

José Sasián

College of Optical Sciences, University of Arizona, Tucson, Arizona 85721
(jose.sasian@optics.arizona.edu)

Received 6 November 2009; accepted 11 December 2009;
posted 22 January 2010 (Doc. ID 119625); published 17 March 2010

A sixth-order theory of wave aberrations for axially symmetric systems is developed. Specific formulas for the sixth-order extrinsic and intrinsic wave aberration coefficients are given, as well as relations between pupil and image aberrations. Equations are developed for the wavefront propagation to the sixth order of approximation. The concept of the irradiance function is developed, and the second-order irradiance coefficients are found via conservation of flux at the pupils of the optical system and in terms of pupil aberrations. From purely geometrical considerations a generalized irradiance transport equation that describes irradiance changes in an optical system is derived. Confirming the aberration coefficients with real ray-tracing data was found to be indispensable. © 2010 Optical Society of America

OCIS codes: 080.1005, 080.1010, 080.2740, 110.2990, 350.5500.

1. Introduction

Aberration theory has been a fruitful field for understanding image formation in optical systems and for designing lens combinations. This paper presents a sixth-order theory of wave aberrations for axially symmetric systems. The paper builds the theory by using Shack's [1] formulation of the aberration function in terms of the field and aperture vectors, Schwarzschild's [3] seminal paper, Hopkins' book on *Wave Theory of Aberrations* [4], Wynne's [5] paper on "Primary aberrations and conjugate change," and Hoffman's [6] Ph.D. dissertation on "Induced aberrations in optical systems." The original goals of the paper have been to provide monochromatic intrinsic and extrinsic coefficients for spherical surfaces while providing insight into and clarity in what has been traditionally an elaborate and perhaps difficult topic. We have tried to simplify the subject by using a minimum of standard notation in theory of wave aberrations, by the form of presentation, and by discussing the physical meaning of the mathematical expressions involved. The goals of the paper have been extended to discuss wave propagation to the sixth order, pupil and image aberration relationships, aspheric surfaces, and connections

to the eikonal function, as well as the little-discussed topic of irradiance variations, or apodization aberrations.

The approach to the subject is first to review the basics of wave aberration theory. Pupil aberrations are interpreted as beam deformations at either pupil. Consequently, as two systems are concatenated and because of pupil distortion, induced or extrinsic aberrations take place. The wavefront deformation on free-space propagation is determined, as well as the wavefront deformation due to the location of the aperture vector. The intrinsic aberration coefficients are theoretically derived when the stop is located at the center of curvature of a spherical surface. When the stop shifts from the center of curvature, the coefficients are found first with the aid of real ray tracing in a semi-empirical manner. Then they are determined with an alternate mathematical form by developing a theory for stop shifting. Attention is given to verifying the correctness of the aberration coefficients. The theory of sixth-order aberrations, in addition to accounting for intrinsic effects, accounts for the wavefront deformation that takes place due to propagation and coordinate changes. These are the new effects that are not considered in fourth-order theory and that provide understanding into the nature of aberrations.

Overall, this work provides some useful insight for understanding how the geometrical wavefront

deforms in propagating through an optical system and contributes to further the theory of imaging aberrations.

2. Goals of Theory of Wave Aberrations

A main goal of the theory of wave aberrations is to determine analytically the geometrical optical field $G(\vec{H}, \vec{\rho})$ at the exit pupil of an optical system, assumed here to be rotationally symmetric and specified by

$$G(\vec{H}, \vec{\rho}) = \sqrt{I_0 \cdot I(\vec{H}, \vec{\rho})} \cdot \exp\left\{-i \frac{2\pi}{\lambda} [n \cdot S(\vec{H}, \vec{\rho}) + W(\vec{H}, \vec{\rho})]\right\}, \quad (1)$$

where $i = \sqrt{-1}$, λ is the wavelength of light, n is the index of refraction of the image space, I_0 is the irradiance at $\vec{H} = 0, \vec{\rho} = 0$, $I(\vec{H}, \vec{\rho})$ is the dimensionless irradiance function, $S(\vec{H}, \vec{\rho})$ is the reference sphere function, and $W(\vec{H}, \vec{\rho})$ is the aberration function. The wave aberration function $W(\vec{H}, \vec{\rho})$ is positive when the wavefront leads the reference sphere. If the aberration function is zero, then the geometrical optical field $G(\vec{H}, \vec{\rho})$ represents in phase a spherical wave.

3. Aberration Function

For an axially symmetric system the aberration function $W(\vec{H}, \vec{\rho})$ provides the geometrical wavefront deformation at the exit pupil as a function of the normalized field \vec{H} and aperture $\vec{\rho}$ vectors. The field vector is located at the object and defines where a given ray originates. The aperture vector is usually located at the exit pupil plane, but it can also be located at the entrance pupil plane. The aperture vector defines the intersection of a given ray with the pupil plane. Figure 1 shows in image space the Gaussian image of the field vector and the aperture vector at the exit pupil plane. The aberration function, being a scalar, involves dot products of the field and aperture vectors, specifically $\vec{H} \cdot \vec{H}$, $\vec{H} \cdot \vec{\rho}$, and $\vec{\rho} \cdot \vec{\rho}$. These dot products depend only on the magnitude of the vectors and the angle ϕ between them and are used to describe axial symmetry; that is, they are invariant on rotation of the coordinate system.

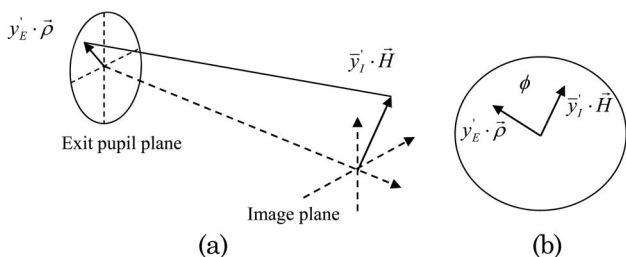


Fig. 1. A, field and aperture vectors (scaled by the marginal ray height at the exit pupil and the chief ray height at the image plane); B, the angle ϕ between them looking down the optical axis.

The aberration function provides the wavefront deformation in terms of optical path as measured along a particular ray and from the reference sphere to the wavefront as shown in Fig. 2. The reference sphere passes by the on-axis exit pupil point, and it is usually centered at the Gaussian image point. The aberration function is written to sixth order as

$$\begin{aligned} W(\vec{H}, \vec{\rho}) &= \sum_{j,m,n} W_{k,l,m} (\vec{H} \cdot \vec{H})^j \cdot (\vec{H} \cdot \vec{\rho})^m \cdot (\vec{\rho} \cdot \vec{\rho})^n \\ &= W_{000} + W_{200}(\vec{H} \cdot \vec{H}) + W_{111}(\vec{H} \cdot \vec{\rho}) \\ &\quad + W_{020}(\vec{\rho} \cdot \vec{\rho}) + W_{040}(\vec{\rho} \cdot \vec{\rho})^2 + W_{131}(\vec{H} \cdot \vec{\rho})(\vec{\rho} \cdot \vec{\rho}) \\ &\quad + W_{222}(\vec{H} \cdot \vec{\rho})^2 + W_{220}(\vec{H} \cdot \vec{H})(\vec{\rho} \cdot \vec{\rho}) \\ &\quad + W_{311}(\vec{H} \cdot \vec{H})(\vec{H} \cdot \vec{\rho}) + W_{400}(\vec{H} \cdot \vec{H})^2 \\ &\quad + W_{240}(\vec{H} \cdot \vec{H})(\vec{\rho} \cdot \vec{\rho})^2 + W_{331}(\vec{H} \cdot \vec{H})(\vec{H} \cdot \vec{\rho})(\vec{\rho} \cdot \vec{\rho}) \\ &\quad + W_{422}(\vec{H} \cdot \vec{H})(\vec{H} \cdot \vec{\rho})^2 + W_{420}(\vec{H} \cdot \vec{H})^2(\vec{\rho} \cdot \vec{\rho}) \\ &\quad + W_{511}(\vec{H} \cdot \vec{H})^2(\vec{H} \cdot \vec{\rho}) + W_{600}(\vec{H} \cdot \vec{H})^3 \\ &\quad + W_{060}(\vec{\rho} \cdot \vec{\rho})^3 + W_{151}(\vec{H} \cdot \vec{\rho})(\vec{\rho} \cdot \vec{\rho})^2 \\ &\quad + W_{242}(\vec{H} \cdot \vec{\rho})^2(\vec{\rho} \cdot \vec{\rho}) + W_{333}(\vec{H} \cdot \vec{\rho})^3, \end{aligned} \quad (2)$$

where the subindices j, m, n represent integer numbers, $k = 2j + m$, $l = 2n + m$, and $W_{k,l,m}$ represent aberration coefficients. This form of the aberration function that uses dot products of the field and aperture vectors is attributed to Shack [1] and is a powerful tool in further development of the theory of wave aberrations. The terms in the aberration function represent aberrations, that is, basic forms in which the wavefront can be deformed. The sum of all aberration terms and orders produces the actual total wavefront deformation. The order of an aberration term is given by $2 \cdot (j + m + n)$, which is always an even order. In the aberration function the field and aperture vectors are normalized so that when they are unity, the coefficients represent the maximum amplitude of each aberration which is expressed in wavelengths. The subindices k, l, m in each coefficient indicate, respectively, the algebraic power of the field vector, the aperture vector, and the cosine of the angle ϕ between these vectors. Table 1 summarizes the first four orders of aberrations, using both vector and

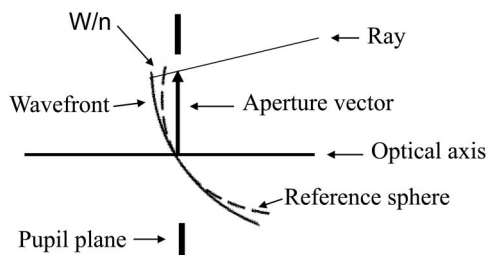


Fig. 2. The tip of the aperture vector defines the intersection of a ray with the pupil plane. The wavefront deformation is the distance along the ray from the reference sphere to the wavefront, and it is negative in this figure.

Table 1. Wavefront Aberrations

Aberration	Vector Form	Algebraic Form	j	m	n
Zero-order					
Uniform piston	W_{000}	W_{000}	0	0	0
Second-order					
Gauss					
Quadratic piston	$W_{200}(\vec{H} \cdot \vec{H})$	$W_{200}H^2$	1	0	0
Magnification	$W_{111}(\vec{H} \cdot \vec{\rho})$	$W_{111}H\rho \cos(\phi)$	0	1	0
Focus	$W_{020}(\vec{\rho} \cdot \vec{\rho})$	$W_{020}\rho^2$	0	0	1
Fourth order					
Seidel					
Spherical aberration	$W_{040}(\vec{\rho} \cdot \vec{\rho})^2$	$W_{040}\rho^4$	0	0	2
Coma	$W_{131}(\vec{H} \cdot \vec{\rho})(\vec{\rho} \cdot \vec{\rho})$	$W_{131}H\rho^3 \cos(\phi)$	0	1	1
Astigmatism	$W_{222}(\vec{H} \cdot \vec{\rho})^2$	$W_{222}H^2\rho^2 \cos^2(\phi)$	0	2	0
Field curvature	$W_{220}(\vec{H} \cdot \vec{H})(\vec{\rho} \cdot \vec{\rho})$	$W_{220}H^2\rho^2$	1	0	1
Distortion	$W_{311}(\vec{H} \cdot \vec{H})(\vec{H} \cdot \vec{\rho})$	$W_{311}H^3\rho \cos(\phi)$	1	1	0
Quartic piston	$W_{400}(\vec{H} \cdot \vec{H})^2$	$W_{400}H^4$	2	0	0
Sixth order					
Schwarzschild					
Oblique spherical aberration	$W_{240}(\vec{H} \cdot \vec{H})(\vec{\rho} \cdot \vec{\rho})^2$	$W_{240}H^2\rho^4$	1	0	2
Coma	$W_{331}(\vec{H} \cdot \vec{H})(\vec{H} \cdot \vec{\rho})(\vec{\rho} \cdot \vec{\rho})$	$W_{331}H^3\rho^3 \cos(\phi)$	1	1	1
Astigmatism	$W_{422}(\vec{H} \cdot \vec{H})(\vec{H} \cdot \vec{\rho})^2$	$W_{422}H^4\rho^2 \cos^2(\phi)$	1	2	0
Field curvature	$W_{420}(\vec{H} \cdot \vec{H})^2(\vec{\rho} \cdot \vec{\rho})$	$W_{420}H^4\rho^2$	2	0	1
Distortion	$W_{511}(\vec{H} \cdot \vec{H})^2(\vec{H} \cdot \vec{\rho})$	$W_{511}H^5\rho \cos(\phi)$	2	1	0
Piston	$W_{600}(\vec{H} \cdot \vec{H})^3$	$W_{600}H^6$	3	0	0
Spherical aberration	$W_{060}(\vec{\rho} \cdot \vec{\rho})^3$	$W_{060}\rho^6$	0	0	3
Unnamed	$W_{151}(\vec{H} \cdot \vec{\rho})(\vec{\rho} \cdot \vec{\rho})^2$	$W_{151}H\rho^5 \cos(\phi)$	0	1	2
Unnamed	$W_{242}(\vec{H} \cdot \vec{\rho})^2(\vec{\rho} \cdot \vec{\rho})$	$W_{242}H^2\rho^4 \cos^2(\phi)$	0	2	1
Unnamed	$W_{333}(\vec{H} \cdot \vec{\rho})^3$	$W_{333}H^3\rho^3 \cos^3(\phi)$	0	3	0

algebraic expressions. The second-order terms are named after Gauss, the fourth-order terms are named Seidel, and the sixth-order terms are named Schwarzschild after their respective seminal papers. The ten sixth-order terms can be divided into two groups. The first group (first six terms) can be considered an improvement on the Seidel terms by their increased field dependence, and the second group (last four terms) represents new wavefront deformation forms. Except for “sixth-order spherical aberration,” the last three terms in the new forms do not have a formal, or widely recognized, name. Figure 3 shows the shape (aperture dependence only) of the zero, second, fourth, and the new wavefront shapes of the sixth-order aberrations.

The piston terms represent a uniform phase change over the aperture and therefore do not degrade the image quality. The second-order terms represent departures from Gaussian imaging, and these coefficients are set to zero. We emphasize that in this work it is assumed that there are no second-order terms in the aberration function. It is a mark of aberration theory that aberration coefficients for the Seidel aberrations, and higher-order, are calculated from paraxial quantities derived from a paraxial marginal and ray chief traces. The fourth-order aberration coefficients are given in Table 2 in terms of the famous Seidel sums $S_I, S_{II}, S_{III}, S_{IV}, S_V$. The calculation of the aberration coefficients requires several quantities that are obtained from tracing a paraxial marginal ray and a paraxial chief ray. These quantities are given in Table 3, where unbarred quantities refer to the marginal ray and barred quantities to the chief ray. The marginal ray height and slope at the

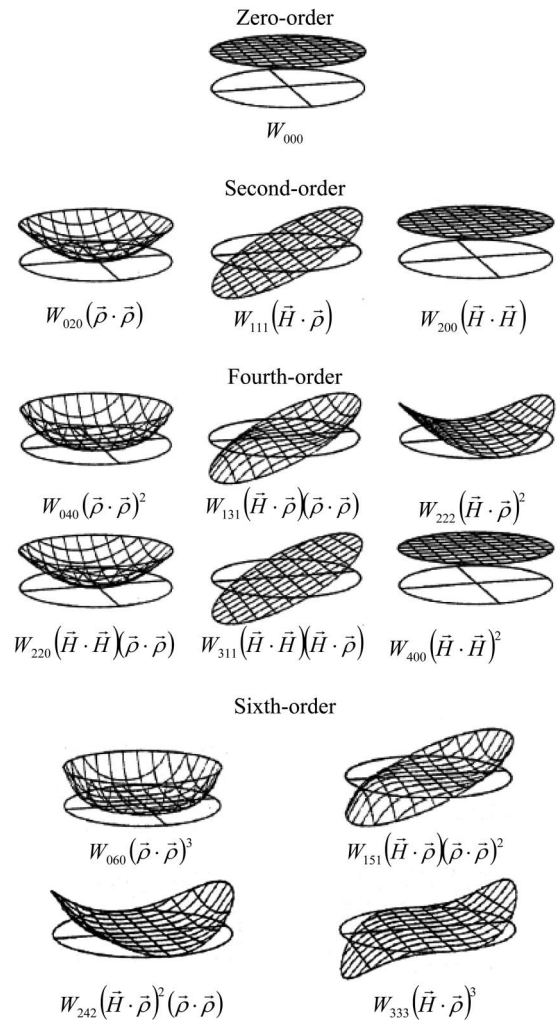


Fig. 3. Wavefront aberration shapes.

Table 2. Seidel Aberration Coefficients

Aberration	Seidel Sum
$W_{040} = \frac{1}{8}S_I$	$S_I = -\sum A^2y\Delta\left(\frac{u}{n}\right)$
$W_{131} = \frac{1}{2}S_{II}$	$S_{II} = -\sum A\bar{A}y\Delta\left(\frac{u}{n}\right)$
$W_{222} = \frac{1}{2}S_{III}$	$S_{III} = -\sum \bar{A}^2y\Delta\left(\frac{u}{n}\right)$
$W_{220} = \frac{1}{4}S_{IV}$	$S_{IV} = -\sum \Psi^2P - \sum \bar{A}^2y\Delta\left(\frac{u}{n}\right)$
$W_{311} = \frac{1}{2}S_V$	$S_V = -\sum \frac{\bar{A}}{A} \left[\Psi^2P + \bar{A}^2y\Delta\left(\frac{u}{n}\right) \right],$ $S_V = -\sum \bar{A} \left[\bar{A}^2\Delta\left(\frac{1}{n^2}\right)y - (\Psi + \bar{A}y)yP \right]$
$W_{400} = \frac{1}{8}S_{VI}$	$S_{VI} = -\sum \bar{A}^2\bar{y}\Delta\left(\frac{u}{n}\right)$

surface in question are y and u , and the chief ray height and slope are \bar{y} and \bar{u} . The radius of curvature of the surface is r . The symbol $\Delta(\cdot)$ stands for the Abbe difference operator, which gives the difference of the quantity inside the parentheses after and before refraction, that is $\Delta(u/n) = u'/n' - u/n$. The summation symbols \sum stand for the sum of the arguments over all the surfaces in the optical system, implying that the aberrations add as expected from knowing that optical paths add. The Seidel sums $S_I, S_{II}, S_{III}, S_{IV}, S_V$ are not in the same form as Seidel produced them, and the sum S_{VI} for piston has been added for completeness. In addition, we have added to S_{IV} the field curvature terms that result from astigmatism and that often are neglected. Table 2 provides an alternate formula for distortion for the case of having the marginal ray normal to the surface, that is $A = 0$. The definition for the Lagrange invariant Ψ used in this paper is opposite in algebraic sign with respect to other works on aberration theory.

4. Pupil Aberrations

When the entrance and exit pupils interchange roles with the object and image, the concept of pupil aberrations arises. The calculation of pupil aberrations is a key in determining how the image aberrations change when the object changes position. An object shift is tantamount to a stop shift in the associated pupil system. From algebraic manipulation Wynne [5] showed that the pupil aberrations are related to the image aberrations by the relationships in Table 4, where pupil aberration coefficients are barred and image aberration coefficients are unbarred. In this table \bar{W}_{220} is the sagittal pupil field curvature and W_{220} is the sagittal image field curva-

ture. In the original work by Wynne the relationship $\bar{W}_{220P} = W_{220P}$ between the pupil and image Petzval field curvature was used, and the relationships were given in terms of Seidel sums. Note that for pupil aberrations the subindices k, l, m in the coefficients $\bar{W}_{k,l,m}$ indicate the algebraic power of ρ, H and $\cos(\phi)$, respectively, rather than of H, ρ , and $\cos(\phi)$ as in the image aberration coefficients $W_{k,l,m}$.

The piston of the image $W_{400}(\bar{H} \cdot \bar{H})^2$ is the optical path difference between the chief ray and the on-axis ray. The optical path for each of these rays is measured from the entrance pupil on-axis point to a reference sphere centered at the exit pupil on-axis point and that passes by the on-axis image point. The optical path difference is a function of the field of view and is equal to the spherical aberration of the pupil $\bar{W}_{040}(\bar{H} \cdot \bar{H})^2$. This definition for piston of the image is somehow arbitrary and is used given the equality relation between spherical aberration of the pupil and piston of the image.

An alternate way to derive the relationships in Table 4 is to consider Fig. 4, which shows the object and image planes OH and $O'H'$, the entrance and exit pupil planes ER and $E'R'$, the reference spheres EA and $E'A'$ for the object and image points H and H' , the reference spheres OB and $O'B'$ for the entrance and exit pupil points R and R' , image wavefront $E'C'$, pupil wavefront $O'D'$, ray $HRR'H'$ from the object point H to the image point H' , ray $ORR'O'$ from the on axis object point to the on-axis image point, and ray $HEE'H'$ from the object point H to the image point H' . The image wavefront deformation $W = n' \cdot A'C'$ at the exit pupil is the segment $C'A'$ multiplied by the index of refraction in image space n' , and the pupil wavefront deformation $\bar{W} = n' \cdot B'D'$ at the image plane is segment $D'B'$ multiplied by the index of refraction in image space n' . Not shown are the ray segments between points R and R' at the pupil planes.

The pupil aberration function $\bar{W}(\bar{H}, \bar{\rho})$ gives the difference in optical path of ray segment $BRR'D'$ with respect to the optical path of ray segment $ORR'O'$. The image aberration function $W(\bar{H}, \bar{\rho})$ gives the difference in optical path of ray segment $ARR'C'$ with respect to the optical path of ray segment $EE'E'H'$. Let us define the reference sphere function $S(\bar{H}, \bar{\rho}) = n \cdot RA$ as the optical path between points RA , and similarly the function $S'(\bar{H}, \bar{\rho}) = n' \cdot R'A'$ as the optical path between points $R'A'$.

Table 3. Quantities Derived from Paraxial Data used in Computing Aberration Coefficients

Quantity	Formula
Refraction-invariant marginal ray	$A = ni = nu + nyc$
Refraction-invariant chief ray	$\bar{A} = n\bar{i} = n\bar{u} + n\bar{y}c$
Lagrange invariant	$\Psi = n\bar{u}y - nu\bar{y} = \bar{A}y - A\bar{y}$
Surface curvature	$c = \frac{1}{r}$
Petzval sum term	$P = c \cdot \Delta\left(\frac{1}{n}\right)$

Table 4. Pupil Aberrations

Name	Identity between Pupil and Image Aberration Coefficients
Pupil spherical aberration	$\bar{W}_{040} = W_{400}$
Pupil coma	$\bar{W}_{131} = W_{311} + \frac{1}{2}\Psi \cdot \Delta\{\bar{u}^2\}$
Pupil astigmatism	$\bar{W}_{222} = W_{222} + \frac{1}{2}\Psi \cdot \Delta\{u\bar{u}\}$
Pupil sagittal field curvature	$\bar{W}_{220} = W_{220} + \frac{1}{4}\Psi \cdot \Delta\{u\bar{u}\}$
Pupil distortion	$\bar{W}_{311} = W_{131} + \frac{1}{2}\Psi \cdot \Delta\{u^2\}$
Pupil piston	$\bar{W}_{400} = W_{040}$

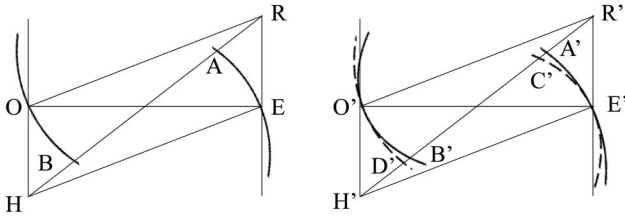


Fig. 4. Schematic for deriving the relationship among the aberration function, the pupil function, and the sphere function.

Then we can write, to within the fourth order of approximation,

$$\bar{W}^{(4)}(\vec{H}, \vec{\rho}) + n \cdot S^{(4)}(\vec{H}, \vec{\rho}) = W^{(4)}(\vec{H}, \vec{\rho}) + n' \cdot S'^{(4)}(\vec{H}, \vec{\rho}). \quad (3)$$

If there are no pupil aberrations, $\bar{W} = 0$; then there is no phase difference in imaging the pupil points R and R' . In this case Eq. (3) states that the aberration function is simply the difference, $W = +n \cdot S - n' \cdot S'$, of the sphere function in object and image spaces; this is consistent with Fig. 4, as points E and A in the incoming wavefront are in phase, and points E' and C' in the outgoing wavefront are in phase. If there are pupil aberrations the wavefront for pupil points R and R' will have a phase difference that is accounted for by the pupil aberration function in Eq. (3). The fourth-order terms of the reference sphere $S(\vec{H}, \vec{\rho})$ function give the relationship

$$\begin{aligned} & n' \cdot S'^{(4)}(\vec{H}, \vec{\rho}) - n \cdot S^{(4)}(\vec{H}, \vec{\rho}) \\ &= \frac{1}{2} \Psi \cdot \Delta\{u^2\} \cdot (\vec{H} \cdot \vec{\rho})(\vec{\rho} \cdot \vec{\rho}) + \frac{1}{2} \Psi \cdot \Delta\{u\bar{u}\} \\ & \cdot (\vec{H} \cdot \vec{\rho})^2 + \frac{1}{4} \Psi \cdot \Delta\{u\bar{u}\} \cdot (\vec{H} \cdot \vec{H})(\vec{\rho} \cdot \vec{\rho}) \\ & + \frac{1}{2} \Psi \cdot \Delta\{\bar{u}^2\} \cdot (\vec{H} \cdot \vec{H})(\vec{H} \cdot \vec{\rho}), \end{aligned} \quad (4)$$

where we have omitted terms related to spherical aberration and piston. For reference, Appendix A gives the coefficients of the sphere function difference $n' \cdot S'(\vec{H}, \vec{\rho}) - n \cdot S(\vec{H}, \vec{\rho})$ to sixth order. When Eq. (4) is inserted into Eq. (3) and similar terms are compared, then the fourth-order relationships in Table 4 follow. The exceptions are the piston of the image and spherical aberration of the pupil that are defined to be equal to each other. For the particular case of a unit magnification system $n \cdot S^{(4)}(\vec{H}, \vec{\rho}) = n' \cdot S'^{(4)}(\vec{H}, \vec{\rho})$, and therefore the image and the pupil aberration functions are equal to the fourth order; that is,

$$W^{(4)}(\vec{H}, \vec{\rho}) = \bar{W}^{(4)}(\vec{H}, \vec{\rho}). \quad (5)$$

We point out that a simple way to determine the fourth-order terms of the sphere function $S(\vec{H}, \vec{\rho})$ is to locate the stop at a spherical surface and set $n = 0$, $n' = 1$, $r = \infty$ in the Seidel coefficients of the aberration function. This maneuver gives fourth-order terms in the distance between the reference

sphere and the flat surface that coincides with the pupil; this distance is the definition of the reference sphere function.

In a different interpretation Sasian [7] has shown that pupil aberrations provide the mapping error between the entrance and exit pupils. The beam cross section from each field point can be distorted as shown in Fig. 5. When the aperture vector $\vec{\rho}$ is set at the entrance pupil, both paraxial and real rays coincide in intersection points at the entrance pupil plane. In the presence of pupil aberrations, a uniform grid at the entrance pupil ($\Delta\vec{\rho}' = 0$) will appear distorted at the exit pupil by $\Delta\vec{\rho}'$,

$$\begin{aligned} \Delta\vec{\rho}' &= \frac{1}{\Psi} \nabla_H \bar{W}(\vec{H}, \vec{\rho}) \\ &= \frac{1}{\Psi} \cdot \left\{ \begin{aligned} & 4 \cdot \bar{W}_{040}(\vec{H} \cdot \vec{H})\vec{H} + \bar{W}_{131}\{(\vec{H} \cdot \vec{H})\vec{\rho} \\ & + 2 \cdot (\vec{H} \cdot \vec{\rho})\vec{H}\} + 2 \cdot \bar{W}_{222}(\vec{H} \cdot \vec{\rho})\vec{\rho} \\ & + 2 \cdot \bar{W}_{220}(\vec{\rho} \cdot \vec{\rho})\vec{H} + \bar{W}_{311}(\vec{\rho} \cdot \vec{\rho})\vec{\rho} \end{aligned} \right\}. \end{aligned} \quad (6)$$

Conversely, when the aperture vector $\vec{\rho}' = \vec{\rho}$ is set at the exit pupil a uniform grid ($\Delta\vec{\rho}' = 0$) at the exit pupil will appear distorted at the entrance pupil by $\Delta\vec{\rho}$,

$$\begin{aligned} \Delta\vec{\rho} &= -\frac{1}{\Psi} \nabla_H \bar{W}(\vec{H}, \vec{\rho}) \\ &= -\frac{1}{\Psi} \cdot \{ 4 \cdot \bar{W}_{040}(\vec{H} \cdot \vec{H})\vec{H} + \bar{W}_{131}\{(\vec{H} \cdot \vec{H})\vec{\rho} \\ & + 2 \cdot (\vec{H} \cdot \vec{\rho})\vec{H}\} + 2 \cdot \bar{W}_{222}(\vec{H} \cdot \vec{\rho})\vec{\rho} \\ & + 2 \cdot \bar{W}_{220}(\vec{\rho} \cdot \vec{\rho})\vec{H} + \bar{W}_{311}(\vec{\rho} \cdot \vec{\rho})\vec{\rho} \}. \end{aligned} \quad (7)$$

5. Coordinate System Geometry

The choice of coordinate system geometry in the study of sixth-order aberrations is critical, as the aberration coefficients depend on the coordinate system used and on its location. In this paper the field vector \vec{H} is located at the object plane and

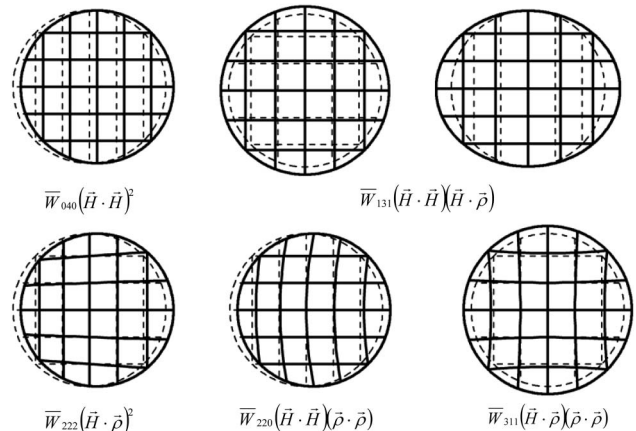


Fig. 5. Pupil grid mapping effects $\Delta\vec{\rho}' = (1/\Psi)\nabla_H \bar{W}(\vec{H}, \vec{\rho})$ due to pupil aberrations in relation to the Gaussian pupil (dashed grid). There is no effect from pupil piston.

indicates the field point from where rays emerge. The aperture vector $\vec{\rho} = \vec{\rho}'$ can be placed either at the entrance pupil plane or at the exit pupil plane, and this will be clarified in the context below. Thus in this paper the coordinate systems for the field and aperture vectors are in planar surfaces that are perpendicular to the system optical axis. The aperture vector is common to all field points, and it indicates the intersection point of a given paraxial ray or real ray with the pupil plane. That is, when the aperture vector is at the entrance pupil, both paraxial and real rays are made to coincide in intersection points and a uniform grid at the entrance pupil is distorted at the exit pupil. Conversely, when the aperture vector is located at the exit pupil, both paraxial and real rays are made to coincide in intersection points and a uniform grid at the exit pupil is distorted at the entrance pupil. This grid distortion results from pupil aberrations. The wavefront deformation is determined by a reference sphere. In the treatment of this paper the reference sphere passes by the on-axis pupil point, and the center of the reference sphere is located at the actual intersection of the chief real ray with the Gaussian image plane, and not as is customary at the Gaussian image point.

For the purposes of aberration coefficient verification, setting the aperture vector $\vec{\rho}$ at the entrance pupil implies making the real rays coincide with paraxial rays at the entrance pupil. This is done by having the aperture stop and entrance pupil coincident. Setting the aperture vector $\vec{\rho}$ at the exit pupil implies making the real rays coincide with paraxial rays at the exit pupil. This is done by making the stop aperture and the exit pupil coincident and by using ray aiming. This may not be physically possible, as either pupil might be virtual, but it can be done within an optical design program.

There are other choices of coordinate systems as, for example, on the reference sphere at the exit pupil. However, in this paper we have chosen coordinates in planes perpendicular to the optical axis for three reasons. First, coefficients are more easily calculated when the coordinate system is common to all field points. Second, a formal diffraction calculation using angular spectrum theory requires knowledge of the optical field on a plane. Third, the aberration coefficients in this paper describe the actual wavefront fans that lens design programs compute.

6. Extrinsic Aberrations

It is known that high-order aberration coefficients comprise an intrinsic and an extrinsic part. The extrinsic part contributed by an optical surface arises because there is aberration before that surface. In the absence of aberration before an optical surface then the surface contributes only its intrinsic part. Sometimes the extrinsic contribution is also called induced aberration.

Extrinsic or induced aberrations can be explained as resulting from the exit–entrance pupil distortion. Hoffman [6] developed formulas for extrinsic coefficients,

using coordinates on the *reference sphere* at the exit pupil. The treatment below gives the extrinsic coefficients with the aperture vector at the specified *pupil plane* (perpendicular to the optical axis).

Consider two systems, *A* and *B*, with aberration functions $W_A(\vec{H}, \vec{\rho})$ and $W_B(\vec{H}, \vec{\rho})$. Assume that the aberration functions are with the aperture vector at the entrance pupil of each system. If these two systems are combined to form a third system *C*, then the total aberration function $W_C(\vec{H}, \vec{\rho})$ to the sixth order is

$$W_C(\vec{H}, \vec{\rho}) = W_A(\vec{H}, \vec{\rho}) + W_B(\vec{H}, \vec{\rho} + \Delta\vec{\rho}'), \quad (8)$$

where

$$\Delta\vec{\rho}' = \frac{1}{\Psi} \nabla_H \bar{W}_A(\vec{H}, \vec{\rho}) + O^{(5)} \quad (9)$$

is the normalized (by the marginal height y'_{pupil} ray at the exit pupil) transverse ray error at the exit pupil. In Eq. (8) it is necessary to account for the exit pupil distortion $\Delta\vec{\rho}'$ of the first system *A* as it is coupled to the entrance pupil of the second system *B*. This is done by modifying the aperture vector in the second system by the correction term $\Delta\vec{\rho}'$. To account for fourth- and sixth-order terms we can write

$$W_C(\vec{H}, \vec{\rho}) = W^{(4)}_A(\vec{H}, \vec{\rho}) + W^{(6)}_A(\vec{H}, \vec{\rho}) + W^{(4)}_B(\vec{H}, \vec{\rho}) + W^{(6I)}_B(\vec{H}, \vec{\rho}) + W^{(6E)}_B(\vec{H}, \vec{\rho}), \quad (10)$$

where $W^{(4)}_A(\vec{H}, \vec{\rho})$ and $W^{(4)}_B(\vec{H}, \vec{\rho})$ are fourth-order terms, $W^{(6I)}_A(\vec{H}, \vec{\rho})$ and $W^{(6I)}_B(\vec{H}, \vec{\rho})$ are sixth-order intrinsic terms, and $W^{(6E)}_B(\vec{H}, \vec{\rho})$ are sixth-order extrinsic terms. The extrinsic terms $W^{(6E)}_B(\vec{H}, \vec{\rho})$ are obtained by replacing $\vec{\rho}$ with $\vec{\rho} + \Delta\vec{\rho}'$ in $W^{(6I)}_B(\vec{H}, \vec{\rho})$ and retaining the sixth-order terms

$$W^{(6E)}_B(\vec{H}, \vec{\rho}) = W^{(6I)}_B(\vec{H}, \vec{\rho} + \Delta\vec{\rho}') - W^{(6I)}_B(\vec{H}, \vec{\rho}). \quad (11)$$

This approach for obtaining the extrinsic terms relies on recognizing that they result from the exit pupil distortion of system *A*.

An alternative and perhaps not so intuitive approach is to calculate the extrinsic terms by locating the aperture vector at the exit pupil of the complete system *C*. In this case we have the normalized displacement vector $\Delta\vec{\rho}$ at the entrance pupil of system *B* to be

$$\Delta\vec{\rho} = -\frac{1}{\Psi} \nabla_H \bar{W}_B(\vec{H}, \vec{\rho}) + O^{(5)}. \quad (12)$$

The aberration function for the combination of systems *A* and *B* into system *C* to sixth order is

$$W_C(\vec{H}, \vec{\rho}) = W^{(4)}_A(\vec{H}, \vec{\rho} + \Delta\vec{\rho}) + W^{(6I)}_A(\vec{H}, \vec{\rho}) + W^{(4)}_B(\vec{H}, \vec{\rho}) + W^{(6I)}_B(\vec{H}, \vec{\rho}). \quad (13)$$

The extrinsic terms $W_B^{6E}(\vec{H}, \vec{\rho})$ due to system B result from the entrance pupil distortion of system B and are obtained by replacing $\vec{\rho}$ with $\vec{\rho} + \Delta\vec{\rho}$ in $W_A^4(\vec{H}, \vec{\rho})$ and retaining the sixth-order terms. This is

$$W_B^{6E}(\vec{H}, \vec{\rho}) = W_A^4(\vec{H}, \vec{\rho} + \Delta\vec{\rho}) - W_A^4(\vec{H}, \vec{\rho}). \quad (14)$$

The extrinsic sixth-order terms $W^{6E}(\vec{H}, \vec{\rho})$ locating the aperture vector at the entrance or exit pupil of the complete system C are given in Table 5. The lower index E in the coefficients has been added to indicate that the coefficients are extrinsic. The upper index $-$ or $+$ has also been added to indicate that the coefficients are with the aperture vector at the entrance pupil ($-$) or at the exit pupil ($+$).

The additional terms ΔW_{331E} , ΔW_{422E} , ΔW_{420E} , and ΔW_{511E} were found by trial and error and by comparison with the results of computer ray tracing as explained below. The presence of these terms is explained as follows. The actual verification of the coefficients by ray tracing in a lens design program set the reference sphere at the intersection of the chief real ray with the Gaussian image plane and not at the Gaussian image point. Thus in the case of using $\vec{\rho}$ at the exit pupil and with the presence of distortion in system A , there is a correction term in the field vector used in the function $S(\vec{H}, \vec{\rho})$ and $S'(\vec{H}, \vec{\rho})$. The field vector must be replaced, in object and image spaces, by $\vec{H} + \frac{1}{\Psi} W_{311}^A(\vec{H} \cdot \vec{H})\vec{\rho}$ to account for the fact that the object point for system B is not at the Gaussian object point defined by \vec{H} and to account for the fact that the reference sphere is not centered at the Gaussian image point. After substitution of the above shifted vector in the fourth-order terms of the function $S(\vec{H}, \vec{\rho})$ and with the aperture vector at the exit pupil, then the sixth-order relationships

for ΔW_{331E} , ΔW_{422E} , ΔW_{420E} , and ΔW_{511E} result. The relationships for ΔW_{331} , ΔW_{422} , ΔW_{420} , and ΔW_{511} when $\vec{\rho}$ is located at the entrance pupil were written by interchanging the upper indices A and B and changing the algebraic sign.

The relationship for the sixth-order extrinsic terms $W^{6E}(\vec{H}, \vec{\rho})$ can also be rewritten in terms of gradients, and to sixth order they become, for $\vec{\rho}$ at the entrance pupil,

$$\begin{aligned} W^{6E}(\vec{H}, \vec{\rho}) &= W_B^4(\vec{H}, \vec{\rho} + \Delta\vec{\rho}'_A) - W_B^4(\vec{H}, \vec{\rho}) \\ &\approx \nabla_{\rho} W_B^4(\vec{H}, \vec{\rho}) \cdot \Delta\vec{\rho}'_A \\ &= \frac{1}{\Psi} \nabla_{\rho} W_B^4(\vec{H}, \vec{\rho}) \cdot \nabla_H \bar{W}_A^4(\vec{H}, \vec{\rho}), \end{aligned} \quad (15)$$

and, for $\vec{\rho}$ at the exit pupil,

$$\begin{aligned} W^{6E}(\vec{H}, \vec{\rho}) &= W_A^4(\vec{H}, \vec{\rho} + \Delta\vec{\rho}_B) - W_A^4(\vec{H}, \vec{\rho}) \\ &\approx \nabla_{\rho} W_A^4(\vec{H}, \vec{\rho}) \cdot \Delta\vec{\rho}_B \\ &= -\frac{1}{\Psi} \nabla_{\rho} W_A^4(\vec{H}, \vec{\rho}) \cdot \nabla_H \bar{W}_B^4(\vec{H}, \vec{\rho}). \end{aligned} \quad (16)$$

In a different interpretation Eqs. (15) and (16) represent a sixth-order correction in optical path difference due to the real ray displacements from the paraxial rays. That is, induced aberrations are also seen as a correction in optical path due to mismatched coordinates at the pupils.

7. Wavefront Propagation

In this section we derive relationships for the wavefront change on propagation in free space. Consider the eikonal $E(X', Y', Z')$ function that gives the optical path length from a given field point to a given

Table 5. Extrinsic Coefficients for Combination of Systems A and B

With Aperture Vector $\vec{\rho}$ at Entrance Pupil	With Aperture Vector $\vec{\rho}$ at Exit Pupil
$W_{060E}^- = \frac{1}{\Psi} \{4W_{040}^B \bar{W}_{311}^A\}$	$W_{060E}^+ = -\frac{1}{\Psi} \{4W_{040}^A \bar{W}_{311}^B\}$
$W_{151E}^- = \left\{ \frac{1}{\Psi} \{3W_{131}^B \bar{W}_{311}^A + 8W_{040}^B \bar{W}_{220}^A + 8W_{040}^B \bar{W}_{222}^A\} \right\}$	$W_{151E}^+ = -\frac{1}{\Psi} \{3W_{131}^A \bar{W}_{311}^B + 8W_{040}^A \bar{W}_{220}^B + 8W_{040}^A \bar{W}_{222}^B\}$
$W_{242E}^- = \frac{1}{\Psi} \{2W_{222}^B \bar{W}_{311}^A + 4W_{131}^B \bar{W}_{220}^A + 6W_{131}^B \bar{W}_{222}^A + 8W_{040}^B \bar{W}_{131}^A\}$	$W_{242E}^+ = -\frac{1}{\Psi} \{2W_{222}^A \bar{W}_{311}^B + 4W_{131}^A \bar{W}_{220}^B + 6W_{131}^A \bar{W}_{222}^B + 8W_{040}^A \bar{W}_{131}^B\}$
$W_{333E}^- = \frac{1}{\Psi} \{4W_{131}^B \bar{W}_{131}^A + 4W_{222}^B \bar{W}_{222}^A\}$	$W_{333E}^+ = -\frac{1}{\Psi} \{4W_{131}^A \bar{W}_{131}^B + 4W_{222}^A \bar{W}_{222}^B\}$
$W_{240E}^- = \frac{1}{\Psi} \{2W_{131}^B \bar{W}_{220}^A + 2W_{220}^B \bar{W}_{311}^A + 4W_{040}^B \bar{W}_{131}^A\}$	$W_{240E}^+ = -\frac{1}{\Psi} \{2W_{131}^A \bar{W}_{220}^B + 2W_{220}^A \bar{W}_{311}^B + 4W_{040}^A \bar{W}_{131}^B\}$
$W_{331E}^- = \frac{1}{\Psi} \{5W_{131}^B \bar{W}_{131}^A + 4W_{220}^B \bar{W}_{220}^A + 4W_{220}^B \bar{W}_{222}^A + 4W_{222}^B \bar{W}_{220}^A + W_{311}^B \bar{W}_{311}^A + 16W_{040}^B \bar{W}_{040}^A\}$	$W_{331E}^+ = -\frac{1}{\Psi} \{5W_{131}^A \bar{W}_{131}^B + 4W_{220}^A \bar{W}_{220}^B + 4W_{220}^A \bar{W}_{222}^B + 4W_{222}^A \bar{W}_{220}^B + W_{311}^A \bar{W}_{311}^B + 16W_{040}^A \bar{W}_{040}^B\}$
$W_{422E}^- = \frac{1}{\Psi} \{2W_{311}^B \bar{W}_{222}^A + 4W_{220}^B \bar{W}_{131}^A + 6W_{131}^B \bar{W}_{131}^A + 8W_{131}^B \bar{W}_{040}^A\}$	$W_{422E}^+ = -\frac{1}{\Psi} \{2W_{311}^A \bar{W}_{222}^B + 4W_{220}^A \bar{W}_{131}^B + 6W_{131}^A \bar{W}_{131}^B + 8W_{131}^A \bar{W}_{040}^B\}$
$W_{420E}^- = \frac{1}{\Psi} \{2W_{220}^B \bar{W}_{131}^A + 2W_{311}^B \bar{W}_{220}^A + 4W_{131}^B \bar{W}_{040}^A\}$	$W_{420E}^+ = -\frac{1}{\Psi} \{2W_{220}^A \bar{W}_{131}^B + 2W_{311}^A \bar{W}_{220}^B + 4W_{131}^A \bar{W}_{040}^B\}$
$W_{511E}^- = \frac{1}{\Psi} \{3W_{311}^B \bar{W}_{131}^A + 8W_{220}^B \bar{W}_{040}^A + 8W_{222}^B \bar{W}_{040}^A\}$	$W_{511E}^+ = -\frac{1}{\Psi} \{3W_{311}^A \bar{W}_{131}^B + 8W_{220}^A \bar{W}_{040}^B + 8W_{222}^A \bar{W}_{040}^B\}$
$W_{600E}^- = \frac{1}{\Psi} \{4W_{311}^B \bar{W}_{040}^A\}$	$W_{600E}^+ = -\frac{1}{\Psi} \{4W_{311}^A \bar{W}_{040}^B\}$
Added terms when the center of the reference sphere is located at the intersection of the chief ray with the Gaussian image plane	
$\Delta W_{331E}^- = -W_{311}^B \Delta^A \{u^2\}/2$	$\Delta W_{331E}^+ = +W_{311}^A \Delta^B \{u^2\}/2$
$\Delta W_{422E}^- = -W_{311}^B \Delta^A \{u\bar{u}\}$	$\Delta W_{422E}^+ = +W_{311}^A \Delta^B \{u\bar{u}\}$
$\Delta W_{420E}^- = -W_{311}^B \Delta^A \{u\bar{u}\}/2$	$\Delta W_{420E}^+ = +W_{311}^A \Delta^B \{u\bar{u}\}/2$
$\Delta W_{511E}^- = -3W_{311}^B \Delta^A \{\bar{u}^2\}/2$	$\Delta W_{511E}^+ = +3W_{311}^A \Delta^B \{\bar{u}^2\}/2$

point X', Y', Z' of an optical system; here we use transverse coordinates rather than angular coordinates to define the eikonal. The eikonal function satisfies the equation [3]

$$\nabla E(X', Y', Z') \cdot \nabla E(X', Y', Z') = \left[\frac{\partial E(X', Y', Z')}{\partial X'} \right]^2 + \left[\frac{\partial E(X', Y', Z')}{\partial Y'} \right]^2 + \left[\frac{\partial E(X', Y', Z')}{\partial Z'} \right]^2 = n^2, \quad (17)$$

where n is the index of refraction of the corresponding space. Let the eikonal of a system that produces a perfect point image be $S_g(X', Y', Z')$ and the coordinates of the Gaussian image point be Y'_g, Y'_g, Z'_g . Since the function $S_g(X', Y', Z')$ produces a perfect point image Y'_g, Y'_g, Z'_g , using the properties of the eikonal we have

$$\nabla \{S_g(X', Y', Z')\} = \frac{n}{R} [X'_g - X', Y'_g - Y', Z'_g - Z'], \quad (18)$$

where R is the radius of curvature of the reference sphere centered at the Gaussian image point Y'_g, Y'_g, Z'_g .

If the coordinates X', Y', Z' are at the exit pupil of an optical system, then the wave aberration function $W(X', Y', Z')$ is given simply by the difference between the function $S_g(X', Y', Z')$ and the system eikonal $E(X', Y', Z')$. This is

$$W(X', Y', Z') = S_g(X', Y', Z') - E(X', Y', Z'). \quad (19)$$

By inserting Eq. (19) into Eq. (17) we obtain

$$|\nabla E(X', Y', Z')|^2 = |\nabla W(X', Y', Z')|^2 - 2 \cdot \nabla W(X', Y', Z') \cdot \nabla S_g(X', Y', Z') + |\nabla S_g(X', Y', Z')|^2 = n^2. \quad (20)$$

If we locate the point Y'_g, Y'_g, Z'_g at infinity, then $\nabla S_g(X', Y', Z')$ vanishes given that R becomes infinite, and we have

$$\nabla W(X', Y', Z') \cdot \nabla W(X', Y', Z') = n^2, \quad (21)$$

given that in this case $\nabla E(X', Y', Z') = \nabla W(X', Y', Z')$. By use of

$$\frac{\partial W}{\partial Z'} \cong \frac{\Delta Z'}{\Delta Z'}, \quad (22)$$

Eq. (21) can be modified to

$$\Delta Z' W(X', Y') \cong n \left(1 - \frac{1}{2n^2} \left(\left[\frac{\partial W}{\partial X'} \right]^2 + \left[\frac{\partial W}{\partial Y'} \right]^2 \right) \right) \cdot \Delta Z' = n \cdot \Delta Z' - \frac{\Delta Z'}{2n} |\nabla W(X', Y')|^2, \quad (23)$$

where $\Delta Z'$ is the distance along the Z' axis that the wavefront has propagated and $\Delta Z' W(X', Y')$ is the

change in wavefront deformation. Equation (23) relates the change of wavefront as it propagates to the two-dimensional gradient of the wavefront and is valid for small propagation distances $\Delta Z'$ or for beams with no second-order terms, as we have located the points Y'_g, Y'_g, Z'_g at infinity. However, we are concerned with the wavefront change over long propagation distances and for beams that are converging or diverging.

Let us consider an optical system where a wavefront ensemble is propagating from an initial plane PP to the exit pupil. The chief ray height and marginal ray height at the initial plane are \bar{y} and y , respectively. Using the normalized field \vec{H} and aperture $\vec{\rho}$ vectors, $Y'_{\text{pupil}} = y_{\text{pupil}} \cdot \rho_y$ and $Y'_{PP} = y \cdot \rho_y$ so that $\partial Y'_{\text{pupil}} = y_{\text{pupil}} \cdot \partial \rho_y$, $\partial Y'_{PP} = y \cdot \partial \rho_y$, we can write at the initial plane $y \cdot \nabla W(X'_{PP}, Y'_{PP}) = \nabla_{\rho} W(\vec{H}, \vec{\rho})$ and at the exit pupil plane $y_{\text{pupil}} \cdot \nabla W(X'_{\text{pupil}}, Y'_{\text{pupil}}) = \nabla_{\rho} W(\vec{H}, \vec{\rho})$.

By making the key substitution of replacing $\nabla W(X', Y') \cdot \nabla W(X', Y')$ with $(1/y y_{\text{pupil}}) \nabla_{\rho} W(\vec{H}, \vec{\rho}) \cdot \nabla_{\rho} W(\vec{H}, \vec{\rho})$ so as to change to normalized coordinates and so that the wavefront change on propagation is symmetrical when it propagates forward or backwards, we obtain

$$\Delta Z' W(\vec{H}, \vec{\rho}) \cong n \cdot \Delta Z' - \frac{\Delta Z'}{2n y y_{\text{pupil}}} \nabla_{\rho} W(\vec{H}, \vec{\rho}) \cdot \nabla_{\rho} W(\vec{H}, \vec{\rho}). \quad (24)$$

We can relate the propagation distance $\Delta Z'$ to the marginal and chief ray heights at the initial plane as

$$-\frac{1}{2n y y_{\text{pupil}}} \frac{\Delta Z'}{2\bar{y}} = \frac{1\bar{y}}{2\bar{y}} \frac{\Delta Z'}{n y y_{\text{pupil}}} = \frac{1\bar{y}}{2\bar{u}'} \frac{1}{n y y_{\text{pupil}}} = \frac{1\bar{y}}{2\bar{y}} \frac{1}{\Psi}, \quad (25)$$

and without accounting for the piston term $n \cdot \Delta Z'$, or limiting $\Delta Z'$ to small propagation distances, we obtain

$$\Delta Z' W(\vec{H}, \vec{\rho}) \cong + \frac{1\bar{y}}{2\bar{y}} \frac{1}{\Psi} \nabla_{\rho} W(\vec{H}, \vec{\rho}) \cdot \nabla_{\rho} W(\vec{H}, \vec{\rho}). \quad (26)$$

This is a useful propagation equation and provides to the sixth order of approximation the wavefront deformation change when a wavefront propagates from an initial plane to a final plane, here the exit pupil plane, where $\bar{y}_{\text{pupil}} = 0$, the propagation distance being $\Delta Z' = -\bar{y} \cdot \bar{u}'^{-1}$. Effectively we have converted Eq. (23) that uses absolute coordinates to Eq. (26) that uses normalized coordinates. In doing this conversion we have removed the limitation of small propagation distances via the factor $1/y y_{\text{pupil}}$.

For the case of a wavefront described by $W(\vec{H}, \vec{\rho}) = [(n \cdot y^2)/(n \cdot y^2)](\vec{\rho} \cdot \vec{\rho})$ and propagating a distance $\Delta Z' = R_1 - R_2$, we have that Eq. (24) predicts the wavefront change to be

$$\begin{aligned}
\Delta_Z W(\vec{H}, \vec{\rho}) &= n \cdot \Delta Z' - \frac{n \cdot \Delta Z'}{2y y_{\text{pupil}}} \cdot \frac{y^4}{R_1^2} (\vec{\rho} \cdot \vec{\rho}) \\
&= n \cdot \Delta Z' - \frac{R_1 - R_2}{R_1 R_2} \cdot \frac{n \cdot y^2}{2} (\vec{\rho} \cdot \vec{\rho}) \\
&= n \cdot \Delta Z' - \left\{ \frac{n \cdot y^2}{2R_1} (\vec{\rho} \cdot \vec{\rho}) - \frac{n \cdot y^2}{2R_2} (\vec{\rho} \cdot \vec{\rho}) \right\} \\
&= n \cdot (R_1 - R_2) + \frac{n}{2R_2} (X'^2 + Y'^2) \\
&\quad - \frac{n}{2R_1} (X'^2 + Y'^2), \tag{27}
\end{aligned}$$

in agreement with our understanding of second-order wave propagation. In Eq. (27) we have used the fact that $y/y_{\text{pupil}} = R_1/R_2$ and that R_1 and R_2 are the vertex radii of the quadratic wavefronts.

To interpret Eq. (26), we point out that the term $\Delta Z' \cdot \nabla_{\rho} W(\vec{H}, \vec{\rho}) \cdot \nabla_{\rho} W(\vec{H}, \vec{\rho})/2n^2 y^2$ in Eq. (24) represents to second order the sag $x^2/2\Delta Z'$ of a sphere of radius $\Delta Z'$ at point $x = \Delta Z' |\nabla_{\rho} W(\vec{H}, \vec{\rho})|/ny$. The sag of a sphere of radius $R_2 = R_1 - \Delta Z'$ is $x^2/2R_2$. With $y/y_{\text{pupil}} = R_1/R_2$ the sum of the sags is $x^2 y/2\Delta Z' y_{\text{pupil}}$, which leads to the term $\Delta Z' \cdot \nabla_{\rho} W(\vec{H}, \vec{\rho}) \cdot \nabla_{\rho} W(\vec{H}, \vec{\rho})/2n^2 y y_{\text{pupil}}$. Thus Eq. (26) gives the change of wavefront deformation as the sum of the sags at the destination plane of a sphere of radius $\Delta Z' = R_1 - R_2$ and a sphere of radius R_2 at point $x = \Delta Z' |\nabla_{\rho} W(\vec{H}, \vec{\rho})|/ny$. This point is simply the transverse deviation at the destination plane of the actual ray.

Equation (26) is significant in that it shows to sixth order how a wavefront ensemble, i.e., the plurality of wavefronts traveling from an extended source, changes as it propagates in free space the distance $\Delta Z'$, which is not limited to be small. This equation provides the geometrical wavefront change, and it does not account for diffraction effects. We assume that the beams are unclipped by an aperture before they reach the exit pupil that coincides with the stop aperture. The terms that result from Eq. (26) are highlighted in Table 6.

8. Wavefront Change with Aperture Vector Location

In this section we show how the aberration coefficients change when the aperture vector is changed from the entrance pupil to the exit pupil. Let us consider the geometry in Fig. 6, which shows the principal planes, the pupil planes, propagating rays, and the object and image planes of an optical system. Generally at the rear principal plane the intersection point of a ray may not coincide with the corresponding intersection at the front principal plane. That is, due to aberration in the system there is coordinate distortion between the principal planes. The difference in intersection points is given by the displacement vector $\Delta \vec{\Omega}$, which is normalized by the marginal ray height y_{PP} at the principal plane. We are interested in describing the wavefront deformation with the aperture vector at the exit pupil. This requires real

Table 6. Wavefront Change at the Exit Pupil on Propagation in Free Space the Distance $\Delta Z' = -\vec{y} \cdot \vec{u}^{-1}$ from the Pupil^a

$\Delta_Z W^-(\vec{H}, \vec{\rho})$	$= \frac{1}{2} \frac{y}{y_{\text{pupil}}} \frac{1}{\Psi} \nabla_{\rho} W(\vec{H}, \vec{\rho}) \cdot \nabla_{\rho} W(\vec{H}, \vec{\rho})$
ΔW_{060}^-	$= \frac{1}{2} \frac{y}{y_{\text{pupil}}} \frac{1}{\Psi} \{16W_{040} W_{040}\}$
ΔW_{151}^-	$= \frac{1}{2} \frac{y}{y_{\text{pupil}}} \frac{1}{\Psi} \{24W_{040} W_{131}\}$
ΔW_{242}^-	$= \frac{1}{2} \frac{y}{y_{\text{pupil}}} \frac{1}{\Psi} \{16W_{040} W_{222} + 8W_{131} W_{131}\}$
ΔW_{240}^-	$= \frac{1}{2} \frac{y}{y_{\text{pupil}}} \frac{1}{\Psi} \{16W_{040} W_{220} + W_{131} W_{131}\}$
ΔW_{333}^-	$= \frac{1}{2} \frac{y}{y_{\text{pupil}}} \frac{1}{\Psi} \{8W_{131} W_{222}\}$
ΔW_{331}^-	$= \frac{1}{2} \frac{y}{y_{\text{pupil}}} \frac{1}{\Psi} \{8W_{040} W_{311} + 4W_{131} W_{222} + 12W_{131} W_{220}\}$
ΔW_{422}^-	$= \frac{1}{2} \frac{y}{y_{\text{pupil}}} \frac{1}{\Psi} \{4W_{131} W_{311} + 4W_{222} W_{222} + 8W_{222} W_{220}\}$
ΔW_{420}^-	$= \frac{1}{2} \frac{y}{y_{\text{pupil}}} \frac{1}{\Psi} \{4W_{220} W_{220} + 2W_{311} W_{131}\}$
ΔW_{511}^-	$= \frac{1}{2} \frac{y}{y_{\text{pupil}}} \frac{1}{\Psi} \{4W_{222} W_{311} + 4W_{220} W_{311}\}$
ΔW_{600}^-	$= \frac{1}{2} \frac{y}{y_{\text{pupil}}} \frac{1}{\Psi} \{W_{311} W_{311}\}$

^aThe aperture vector is at the initial propagation plane.

rays to pass by the object point and to coincide with paraxial rays at the exit pupil. As shown in Fig. 6 requiring real rays to coincide with paraxial rays at the exit pupil changes their intersection point at the exit pupil by $-y'_{\text{pupil}} \cdot \Delta \vec{\rho}'$, at the rear principal plane by $y_{PP} \cdot \Delta \vec{\rho}$, and at the entrance pupil by $y_{\text{pupil}} \cdot \Delta \vec{\rho}$.

The wavefront change $W^+(\vec{H}, \vec{\rho}) - W^-(\vec{H}, \vec{\rho})$ when the aperture vector is changed from the entrance to the exit pupil is found by replacing $\vec{\rho}$ by $\vec{\rho} + \Delta \vec{\rho}$ in the fourth-order terms of the aberration function and retaining the resulting sixth-order terms. Using the gradient operator, this is

$$\begin{aligned}
W^+(\vec{H}, \vec{\rho}) - W^-(\vec{H}, \vec{\rho}) &= \nabla_{\rho} \{W(\vec{H}, \vec{\rho}) \\
&\quad - W_{311}(\vec{H} \cdot \vec{H})(\vec{H} \cdot \vec{\rho})\} \\
&\quad \cdot \Delta \vec{\rho} = -\frac{1}{\Psi} \nabla_{\rho} W(\vec{H}, \vec{\rho}) \\
&\quad \cdot \nabla_H \bar{W}(\vec{H}, \vec{\rho}) - \frac{1}{\Psi} \nabla_{\rho} W_{311}(\vec{H} \cdot \vec{H}) \\
&\quad \times (\vec{H} \cdot \vec{\rho}) \cdot \nabla_H \bar{W}(\vec{H}, \vec{\rho}), \tag{28}
\end{aligned}$$

where we have subtracted distortion $W_{311}(\vec{H} \cdot \vec{H})(\vec{H} \cdot \vec{\rho})$ as the reference sphere is centered at the actual intersection of the chief ray with the Gaussian image plane.

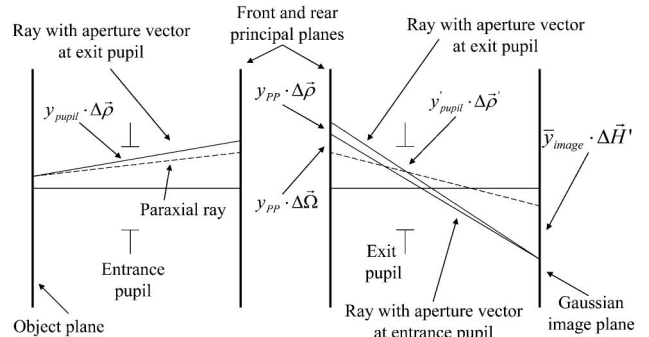


Fig. 6. Construction for deriving the relationship $\Delta \vec{\Omega} = (y_{PP}/y_{PP}) \Delta \vec{H}' - \Delta \vec{\rho}$.

The sixth-order terms involved in $-\frac{1}{\Psi} \nabla_{\rho} W(\vec{H}, \vec{\rho}) \cdot \nabla_H \bar{W}(\vec{H}, \vec{\rho})$ are highlighted in Table 7 as they give the wavefront difference between having the aperture vector at the entrance and exit pupils for the case of centering the reference at the Gaussian image point.

9. Displacement Vector $\Delta \vec{\Omega}$ and Image and Pupil Aberration Functions

In this section we relate the displacement vector $\Delta \vec{\Omega}$ at the principal plane to the gradients of the image and pupil aberration functions. From Fig. 6 we can establish the equality

$$\Delta \vec{\rho} + \Delta \vec{\Omega} = -\frac{\Delta Z}{l - \Delta Z} \frac{\bar{y}_{\text{image}}}{y_{PP}} \Delta \vec{H}' = \frac{\bar{y}_{PP}}{y_{PP}} \Delta \vec{H}', \quad (29)$$

where l is the distance from the rear principal plane to the image plane and $\Delta \vec{H}'$ is the normalized (by the image height \bar{y}_{image}) transverse ray intercept error at the image plane, given by

$$\begin{aligned} \Delta \vec{H}' &= \frac{1}{\bar{y}_{\text{image}} n' u'} \nabla_{\rho} W(\vec{H}, \vec{\rho}) + O^{(5)} \\ &= -\frac{1}{\Psi} \nabla_{\rho} W(\vec{H}, \vec{\rho}) + O^{(5)}. \end{aligned} \quad (30)$$

Then the displacement vector $\Delta \vec{\Omega}$ that gives the ray mapping error between the principal planes is

$$\begin{aligned} \Delta \vec{\Omega} &= \frac{\bar{y}_{PP}}{y_{PP}} \Delta \vec{H}' - \Delta \vec{\rho} \\ &= \frac{1}{\Psi} \left[\nabla_H \bar{W}(\vec{H}, \vec{\rho}) - \frac{\bar{y}_{PP}}{y_{PP}} \nabla_{\rho} W(\vec{H}, \vec{\rho}) \right]. \end{aligned} \quad (31)$$

To illustrate these results, consider the following example. Algebraic manipulation of the aberration coefficients for a single spherical surface permits writing the relationships in Table 8. The coefficients W_{311}^0 and \bar{W}_{311}^0 represent the distortion between the uniform paraxial coordinates at the front principal plane and the actual distorted coordinates at the rear principal plane of the surface. For a flat surface the coefficients W_{311}^0 and \bar{W}_{311}^0 vanish, $\Delta \vec{\Omega} = 0$,

and the simple relationship $(\bar{y}_{PP}/y_{PP}) \nabla_{\rho} W(\vec{H}, \vec{\rho}) = \nabla_H \bar{W}(\vec{H}, \vec{\rho})$ between the gradients of the image and pupil aberrations follows. This can be verified term by term by using Tables 6 and 7.

10. Wavefront Propagation to Sixth-Order Approximation in an Optical System

In this section we summarize the previous results. As a geometrical wavefront propagates in free space the Gaussian properties and the fourth-order wavefront aberration coefficients remain the same. However, sixth-order properties change. To sixth order the wavefront change $\Delta_Z W(\vec{H}, \vec{\rho})$ on free-space propagation is given by

$$\Delta_Z W(\vec{H}, \vec{\rho}) = \pm \frac{1}{2} \frac{\bar{y}}{y} \frac{1}{\Psi} \nabla_{\rho} W(\vec{H}, \vec{\rho}) \cdot \nabla_{\rho} W(\vec{H}, \vec{\rho}), \quad (32)$$

where the propagation distance is $\Delta Z' = \bar{y} \cdot \bar{u}'^{-1}$. The positive sign is for having the aperture vector at the initial plane, and the negative sign is for having the aperture vector at the destination plane.

The sixth-order wavefront change $\Delta_Z W(\vec{H}, \vec{\rho})$ on coordinate distortion is

$$\Delta_Z W(\vec{H}, \vec{\rho}) = \nabla_{\rho} W(\vec{H}, \vec{\rho}) \cdot \Delta \vec{\varepsilon}, \quad (33)$$

where $\Delta \vec{\varepsilon}$ is the coordinate distortion and $W(\vec{H}, \vec{\rho})$ is the wavefront deformation at the plane of the distortion.

The change of wavefront on changing the aperture vector from the entrance to the exit pupil and having the reference sphere centered at the Gaussian image points is

$$W^+(\vec{H}, \vec{\rho}) - W^-(\vec{H}, \vec{\rho}) = -\frac{1}{\Psi} \nabla_{\rho} W(\vec{H}, \vec{\rho}) \cdot \nabla_H \bar{W}(\vec{H}, \vec{\rho}). \quad (34)$$

Extrinsic aberrations as a result of combining two optical systems A and B and having the reference sphere centered at the Gaussian image point are, for $\vec{\rho}$ at the entrance pupil,

Table 7. Change in Wavefront on Placing the Aperture Vector at the Exit Pupil^a

$W^+(\vec{H}, \vec{\rho}) - W^-(\vec{H}, \vec{\rho}) = -\frac{1}{\Psi} \nabla_{\rho} W(\vec{H}, \vec{\rho}) \cdot \nabla_H \bar{W}(\vec{H}, \vec{\rho})$
$W_{060}^+ - W_{060}^- = -\frac{1}{\Psi} \{4W_{040} \bar{W}_{311}\}$
$W_{151}^+ - W_{151}^- = -\frac{1}{\Psi} \{3W_{131} \bar{W}_{311} + 8W_{040} \bar{W}_{220} + 8W_{040} \bar{W}_{222}\}$
$W_{242}^+ - W_{242}^- = -\frac{1}{\Psi} \{2W_{222} \bar{W}_{311} + 4W_{131} \bar{W}_{220} + 6W_{131} \bar{W}_{222} + 8W_{040} \bar{W}_{131}\}$
$W_{333}^+ - W_{333}^- = -\frac{1}{\Psi} \{4W_{131} \bar{W}_{131} + 4W_{222} \bar{W}_{222}\}$
$W_{240}^+ - W_{240}^- = -\frac{1}{\Psi} \{2W_{131} \bar{W}_{220} + 2W_{220} \bar{W}_{311} + 4W_{040} \bar{W}_{131}\}$
$W_{331}^+ - W_{331}^- = -\frac{1}{\Psi} \{5W_{131} \bar{W}_{131} + 4W_{220} \bar{W}_{220} + 4W_{220} \bar{W}_{222} + 4W_{222} \bar{W}_{220} + W_{311} \bar{W}_{311} + 16W_{040} \bar{W}_{040}\}$
$W_{422}^+ - W_{422}^- = -\frac{1}{\Psi} \{2W_{311} \bar{W}_{222} + 4W_{220} \bar{W}_{131} + 6W_{222} \bar{W}_{131} + 8W_{131} \bar{W}_{040}\}$
$W_{420}^+ - W_{420}^- = -\frac{1}{\Psi} \{2W_{220} \bar{W}_{131} + 2W_{311} \bar{W}_{220} + 4W_{131} \bar{W}_{040}\}$
$W_{511}^+ - W_{511}^- = -\frac{1}{\Psi} \{3W_{311} \bar{W}_{131} + 8W_{220} \bar{W}_{040} + 8W_{222} \bar{W}_{040}\}$
$W_{600}^+ - W_{600}^- = -\frac{1}{\Psi} \{4W_{311} \bar{W}_{040}\}$

^aThe reference sphere is centered at the Gaussian image point.

Table 8. Image and Pupil Coefficient Relationships for a Spherical Surface

$4W_{040} \frac{y}{r} = \bar{W}_{311} - \bar{W}_{311}^0$	$4\bar{W}_{040} \frac{y}{r} = W_{311} - W_{311}^0$
$W_{131} \frac{y}{r} = \bar{W}_{222} - \bar{W}_{311}^0 \frac{y}{r}$	$\bar{W}_{131} \frac{y}{r} = W_{222} - W_{311}^0 \frac{y}{r}$
$W_{222} \frac{y}{r} = \bar{W}_{131} + W_{311}^0$	$\bar{W}_{222} \frac{y}{r} = W_{131} + \bar{W}_{311}^0$
$W_{220} \frac{y}{r} = \frac{1}{2} \bar{W}_{131} - \frac{1}{2} \bar{W}_{311}^0 \left(\frac{y}{r}\right)^2$	$\bar{W}_{220} \frac{y}{r} = \frac{1}{2} W_{131} - \frac{1}{2} W_{311}^0 \left(\frac{y}{r}\right)^2$
$W_{311} \frac{y}{r} = 4\bar{W}_{040} + W_{311}^0 \frac{y}{r}$	$\bar{W}_{311} \frac{y}{r} = 4W_{040} + \bar{W}_{311}^0 \frac{y}{r}$
$W_{311}^0 = W_{311}^{y=0} = \frac{1}{2R} \Psi \bar{A} y \Delta \left\{ \frac{1}{n} \right\} = \frac{1}{2} \Psi \bar{\alpha} (u' - u)$	$\bar{W}_{311}^0 = \bar{W}_{311}^{y=0} = -\frac{1}{2R} \Psi A y \Delta \left\{ \frac{1}{n} \right\} = -\frac{1}{2} \Psi \alpha (u' - u)$
$\alpha = \frac{y}{r}$	$\bar{\alpha} = \frac{y}{r}$

$$W_E^-(\vec{H}, \vec{\rho}) = \frac{1}{\Psi} \nabla_\rho W_B(\vec{H}, \vec{\rho}) \cdot \nabla_H \bar{W}_A(\vec{H}, \vec{\rho}), \quad (35)$$

and, for $\vec{\rho}$ at the exit pupil,

$$W_E^+(\vec{H}, \vec{\rho}) = -\frac{1}{\Psi} \nabla_\rho W_A(\vec{H}, \vec{\rho}) \cdot \nabla_H \bar{W}_B(\vec{H}, \vec{\rho}). \quad (36)$$

11. Intrinsic Aberrations

Intrinsic aberrations are the aberrations that an optical surface contributes when the incoming light beam has no aberrations. That is, we assume that the object for that optical surface lies on a flat surface and that the individual wavefronts arriving at the surface are spherical. In this section we provide the intrinsic aberration coefficients for spherical surfaces. The derivation is based on theory for contributions at a stop at the center of curvature. Stop shifting proved to be difficult to unveil, and so the contributions on stop shifting were found with the aid of a computer. However, Appendices B and C show, on a theoretical basis, the process of stop shifting for both an aspheric surface and a spherical surface. We have chosen the present order of providing the results because it is the manner in which they were obtained.

A. Sixth-Order Spherical Aberration W_{060}

The intrinsic sixth-order wave aberration coefficient for spherical aberration from a spherical surface with the stop at the surface has been given by Sasian [8] and is

$$W_{060}^- = 4W_{040} \left[\frac{1y^2}{8r^2} - \frac{1}{8} A \left(\frac{u'}{n'} + \frac{u}{n} \right) + \frac{1y}{2r} u \right], \quad (37)$$

where the term $\frac{1}{2}(y/r)u$ has been added to account for the difference in intercepts between the marginal paraxial ray and the real ray intersection at the surface required in the original formula; r is the radius of curvature of the surface. For completeness, Appendix D provides a derivation of coefficients used in this section. Equation (37) is with the aperture stop at the surface and with the aperture vector at the entrance pupil. Unless specified aberration coefficients with the aperture vector at the entrance pupil are marked with a $-$ upper index as W^- , and aberration coefficients with the aperture vector at the exit pupil

are marked with a $+$ upper index as W^+ . If the stop is shifted to a different location, because of free-space propagation and fourth-order spherical aberration, there will be a contribution to sixth-order spherical aberration as a transfer term. Using Eq. (26), we have that the transfer term is

$$W_{060}^{\text{transfer}} = \frac{8}{\Psi} W_{040} \cdot W_{040} \frac{y}{r}, \quad (38)$$

and the total intrinsic coefficient is

$$W_{060I}^- = W_{040} \left[\frac{1y^2}{2r^2} - \frac{1}{2} A \left(\frac{u'}{n'} + \frac{u}{n} \right) + 2\frac{y}{r} u \right] + \frac{8}{\Psi} W_{040} \cdot W_{040} \frac{y}{r}, \quad (39)$$

where the lower index I has been added to indicate that the coefficient is intrinsic. If the wavefront propagates in reverse from the exit pupil to the entrance pupil, we have that this is equivalent to having the aperture vector at the exit pupil. Therefore the sixth-order coefficient for spherical aberration with the aperture vector at the exit pupil is

$$W_{060I}^+ = W_{040} \left[\frac{1y^2}{2r^2} - \frac{1}{2} A \left(\frac{u'}{n'} + \frac{u}{n} \right) + 2\frac{y}{r} u' \right] - \frac{8}{\Psi} W_{040} \cdot W_{040} \frac{y}{r}, \quad (40)$$

where the difference between W_{060I}^- and W_{060I}^+ is the use of the marginal ray slope u' in image space rather than slope u in object space and the change of sign in the transfer term. Furthermore, since

$$\frac{4}{\Psi} W_{040} \bar{W}_{311}^0 = -2W_{040} \frac{y}{r} (u' - u), \quad (41)$$

$$\frac{8}{\Psi} W_{040} W_{040} \frac{y}{r} = \frac{2}{\Psi} W_{040} (\bar{W}_{311} - \bar{W}_{311}^0), \quad (42)$$

then we can also write

$$W_{060I}^+ = W_{060I}^- - \frac{4}{\Psi} W_{040} \bar{W}_{311}. \quad (43)$$

Thus we have two forms for the relationship between coefficients with the aperture vector at the entrance pupil W_{060I}^- and with the aperture vector at the exit pupil W_{060I}^+ . One form uses a change of the ray slopes and a sign change in the transfer term; the other form adds a term that involves products of fourth-order aberrations. This latter term is reminiscent of induced aberrations, and it accounts for the change of coordinates or placement of the aperture vector as discussed in the previous section.

B. Oblique Spherical Aberration W_{240} and Sixth-Order Field Curvature W_{420} with the Stop at the Center of Curvature

We calculate oblique spherical aberration W_{240} and field curvature W_{420} by first locating the aperture stop at the center of curvature of the surface. Spherical aberration W_{040} depends on the conjugate distances s and s' . As shown in Appendix D, these distances vary for off-axis object points, and when the variations are considered the coefficients for W_{240} and W_{420} result. In this derivation there is no distortion and the reference sphere is centered at the Gaussian image point. The lower index CC indicates that the coefficient has the stop at the center of curvature of the surface. Thus for oblique spherical aberration W_{240} we have

$$W_{240CC}^- = + \left[\frac{1}{16} \frac{A}{r} \Psi^2 \Delta \left\{ \frac{u}{n^2} \right\} + \frac{1}{8} \frac{1}{r} \Psi^2 \Delta \left\{ \frac{u^2}{n} \right\} \right. \\ \left. + \frac{1}{4} \frac{y^2}{r^2} W_{220P} + \frac{y}{r} u W_{220P} - \frac{1}{4} \frac{u'}{r} \Psi^2 \Delta \left\{ \frac{u}{n} \right\} \right], \quad (44)$$

$$W_{240CC}^+ = + \left[\frac{1}{16} \frac{A}{r} \Psi^2 \Delta \left\{ \frac{u}{n^2} \right\} + \frac{1}{8} \frac{1}{r} \Psi^2 \Delta \left\{ \frac{u^2}{n} \right\} \right. \\ \left. + \frac{1}{4} \frac{y^2}{r^2} W_{220P} + \frac{y}{r} u' W_{220P} - \frac{1}{4} \frac{u}{r} \Psi^2 \Delta \left\{ \frac{u}{n} \right\} \right], \quad (45)$$

$$W_{240CC}^+ = W_{240CC}^- - \frac{2}{\bar{\Psi}} W_{220P} \cdot \bar{W}_{311} + \frac{2}{\bar{\Psi}} W_{220P} \cdot W_{131}, \quad (46)$$

where the term

$$W_{220P} = -\frac{1}{4} \Psi^2 P = -\frac{1}{4r} \Psi^2 \Delta \left(\frac{1}{n} \right) \quad (47)$$

is the Petzval field curvature. For sixth-order field curvature W_{420} we have

$$W_{420CC}^- = W_{420CC}^+ = \frac{3}{16} \frac{1}{r^3} \Psi^4 \Delta \left\{ \frac{1}{n} \right\} \frac{1}{A^2}. \quad (48)$$

For the case of $A = 0$ we have $W_{420CC}^- = W_{420CC}^+ = 0$ which follows from considering the sagittal Coddington

equation and noting that when $s' = s$ the sagittal field surface must be flat, and so all orders of field curvature W_{k20} are zero.

C. Sixth-Order Astigmatism W_{422} , Coma W_{331} , W_{151} , and W_{242} with the Stop at the Center of Curvature

For off-axis field points the reference sphere is tilted with respect to the exit pupil. This creates a distortion of coordinates that in the presence of spherical aberration and field curvature gives origin to sixth-order terms. Effectively, coordinate distortion induces sixth-order terms as part of the intrinsic terms. These terms are simple products of fourth-order coefficients and the paraxial ray slopes. Specifically, they are

$$W_{331CC}^+ = -2W_{220P} \cdot u' \bar{u}', \quad (49)$$

$$W_{331CC}^- = -2W_{220P} \cdot u \bar{u}, \quad (50)$$

$$W_{422CC}^+ = -W_{220P} \cdot \bar{u}'^2, \quad (51)$$

$$W_{422CC}^- = -W_{220P} \cdot \bar{u}^2, \quad (52)$$

$$W_{151CC}^+ = -4W_{040} \cdot u' \bar{u}', \quad (53)$$

$$W_{151CC}^- = -4W_{040} \cdot u \bar{u}, \quad (54)$$

$$W_{242CC}^+ = -2W_{040} \cdot \bar{u}'^2, \quad (55)$$

$$W_{242CC}^- = -2W_{040} \cdot \bar{u}^2. \quad (56)$$

D. Aberration Coefficients when the Aperture Stop is Shifted from the Center of Curvature

We have that the aberration function to sixth order when the aperture stop is located at the surface center of curvature is

$$W_{CC}^+(\vec{H}, \vec{\rho}) = W_{040}(\vec{\rho} \cdot \vec{\rho})^2 + W_{220}(\vec{H} \cdot \vec{H})(\vec{\rho} \cdot \vec{\rho}) \\ + W_{240CC}^+(\vec{H} \cdot \vec{H})(\vec{\rho} \cdot \vec{\rho})^2 \\ + W_{331CC}^+(\vec{H} \cdot \vec{H})(\vec{H} \cdot \vec{\rho})(\vec{\rho} \cdot \vec{\rho}) \\ + W_{422CC}^+(\vec{H} \cdot \vec{H})(\vec{H} \cdot \vec{\rho})^2 \\ + W_{420CC}^+(\vec{H} \cdot \vec{H})^2(\vec{\rho} \cdot \vec{\rho}) \\ + W_{060}^+(\vec{\rho} \cdot \vec{\rho})^3 + W_{151CC}^+(\vec{H} \cdot \vec{\rho}) \cdot (\vec{\rho} \cdot \vec{\rho})^2 \\ + W_{242CC}^+(\vec{H} \cdot \vec{\rho})^2(\vec{\rho} \cdot \vec{\rho}), \quad (57)$$

where we have not accounted for piston terms and have located the aperture vector at the exit pupil. Stop shifting refers to the process of changing the

location of the aperture stop while maintaining the same Lagrange invariant. This requires the change of the aperture stop size to maintain the same working f -number. As the stop shifts, different portions of the light beams are selected to pass through the stop, and thus the aberrations change. In fourth-order theory a stop shift is performed by substitution of the aperture vector $\vec{\rho}$ for the shifted vector $\vec{\rho}_{\text{shift}}$,

$$\vec{\rho}_{\text{shift}} = \vec{\rho} + \frac{\bar{y}_{OP}}{y_{OP}} \vec{H} = \vec{\rho} + \frac{\bar{A}}{A} \vec{H}, \quad (58)$$

into the fourth-order terms of the aberration function and carrying out the expansion of terms. The quantities y_{OP} and \bar{y}_{OP} are the marginal ray and chief heights at the old stop position, which is at the center of curvature. In sixth-order theory it is also necessary to account for the fact that as the stop is shifted the wavefront propagates and deforms as specified by Eq. (26). In addition, as the reference sphere also shifts position, there is a coordinate distortion to account for and also for the change of the center of the reference sphere as the real ray intersection changes from the Gaussian image point. In accounting for all of these effects it is helpful to have a common exit pupil for all field points and to place the aperture vector at the exit pupil so that no other coordinate distortion effects take place. The coordinate distortion effects are subtle, and formula checking with actual ray tracing as explained below is indispensable.

For oblique spherical aberration W_{240} we have

$$W_{240I}^+ = W_{240CC}^+ + 3 \left(\frac{\bar{A}}{A} \right)^2 W_{060I}^+ - 8 \frac{1}{\bar{\Psi}} \frac{\bar{A}}{A} W_{040} \cdot W_{220P} + W_{222} u'^2 - W_{131} u' \bar{u}'. \quad (59)$$

The term $3(\bar{A}/A)^2 W_{060I}^+$ results from the expansion of $W_{060}^+(\vec{\rho} \cdot \vec{\rho})^6$ when $\vec{\rho} + (\bar{A}/A)\vec{H}$ is substituted; the term $-8(1/\bar{\Psi})(\bar{A}/A)W_{040} \cdot W_{220P}$ results from wavefront propagation, and the terms $W_{222}u'^2 - W_{131}u'\bar{u}'$ result from coordinate distortion.

For sixth-order coma W_{331} we have

$$W_{331I}^+ = 4 \frac{\bar{A}}{A} W_{240I}^+ + 2 \frac{\bar{A}}{A} W_{242CC}^+ + \frac{\bar{A}}{A} W_{220} u'^2 + W_{311} u'^2 - 2W_{220P} u' \bar{u}'. \quad (60)$$

For sixth-order astigmatism W_{422} we have

$$W_{422I}^+ = 4 \left(\frac{\bar{A}}{A} \right)^2 W_{240I}^+ + 2 \frac{\bar{A}}{A} W_{331CC}^+ - 2W_{222} \bar{u}'^2 - W_{220} \bar{u}'^2 + 2 \left(\frac{\bar{A}}{A} \right)^2 W_{220} u'^2 + W_{311} u' \bar{u}' + \frac{1}{2} \frac{\bar{A}}{A} W_{311} u'^2 + 2 \frac{\bar{A}}{A} W_{220} u' \bar{u}'. \quad (61)$$

For sixth-order field curvature W_{420} we have

$$W_{420I}^+ = 3 \left(\frac{\bar{A}}{A} \right)^4 W_{060I}^+ + 2 \left(\frac{\bar{A}}{A} \right)^2 W_{240CC}^+ - 4 \left(\frac{\bar{A}}{A} \right)^2 \frac{1}{\bar{\Psi}} W_{131} \cdot W_{220P} - 2 \frac{\bar{A}}{A} \frac{1}{\bar{\Psi}} W_{220P} \cdot W_{220P} + W_{420CC}^+ + \frac{\bar{A}}{A} W_{331CC}^+ + \left(\frac{\bar{A}}{A} \right)^2 W_{220P} u'^2 + \frac{1}{2} \frac{\bar{A}}{A} W_{311} u'^2 - \frac{1}{2} W_{311} u' \bar{u}' + 2 \frac{\bar{A}}{A} W_{220P} u' \bar{u}' + \left(\frac{\bar{A}}{A} \right)^2 W_{222} u'^2 - \frac{1}{2} W_{222} \bar{u}'^2. \quad (62)$$

For sixth-order distortion W_{511} we have

$$W_{511I}^+ = 6 \left(\frac{\bar{A}}{A} \right)^5 W_{060I}^+ + 4 \left(\frac{\bar{A}}{A} \right)^3 \left[W_{240CC}^+ - 8 \frac{\bar{A}}{A} \frac{1}{\bar{\Psi}} W_{040} \cdot W_{220P} \right] + 2 \frac{\bar{A}}{A} \left[W_{420CC}^+ - 2 \frac{\bar{A}}{A} \frac{1}{\bar{\Psi}} W_{220P} \cdot W_{220P} \right] + \left(\frac{\bar{A}}{A} \right)^3 W_{222} u'^2 + 2 \left(\frac{\bar{A}}{A} \right)^2 W_{311} u'^2 - \left(\frac{\bar{A}}{A} \right)^2 W_{222} u' \bar{u}' - 2 \left(\frac{\bar{A}}{A} \right)^2 W_{220P} u' \bar{u}' - \frac{\bar{A}}{A} W_{222} \bar{u}'^2 + \frac{1}{2} W_{311} \bar{u}'^2. \quad (63)$$

For sixth-order W_{151} we have

$$W_{151I}^+ = 6 \frac{\bar{A}}{A} W_{060I}^+ + W_{131} u'^2 + W_{151CC}^+. \quad (64)$$

For sixth-order W_{242} we have

$$W_{242I}^+ = 12 \left(\frac{\bar{A}}{A} \right)^2 W_{060I}^+ + \frac{7}{2} W_{222} u'^2 - 3W_{131} u' \bar{u}' + W_{242CC}^+. \quad (65)$$

For sixth-order W_{333} we have

$$W_{333I}^+ = 8 \left(\frac{\bar{A}}{A} \right)^3 W_{060I}^+ + 4 \left(\frac{\bar{A}}{A} \right)^2 W_{151CC}^+ + 3 \frac{\bar{A}}{A} W_{222} u'^2 + 2 \frac{\bar{A}}{A} W_{242CC}^+ + 2W_{222} u' \bar{u}', \quad (66)$$

and sixth-order piston W_{600} may be set equal to the sixth-order spherical aberration of the pupil; this is

$$W_{600I}^+ = \bar{W}_{060I}^+. \quad (67)$$

Table 9 summarizes the quantities used for the calculation of the intrinsic coefficients with the aperture vector at the exit pupil. Table 10 summarizes the intrinsic coefficients of a spherical surface with the aperture vector at the exit pupil.

12. Relationships between Coefficients

Table 11 presents the relationships between the sixth-order intrinsic aberrations coefficients W^- and W^+ with the aperture vector at the entrance pupil and at the exit pupil. These were found by using real ray tracing to numerically find the magnitude of the coefficients and by the suggested analogy with the formula development in this paper. After noting that $4W_{220} \cdot \bar{W}_{220} = W_{311} \cdot \bar{W}_{311}$ and that $2W_{311} \cdot \bar{W}_{222} = 4W_{220} \cdot \bar{W}_{131}$, the relationships in Table 11 match the theoretical prediction:

$$\begin{aligned} W_I^+(\vec{H}, \vec{\rho}) - W_I^-(\vec{H}, \vec{\rho}) &= \nabla_{\rho} \{W(\vec{H}, \vec{\rho}) - W_{311}(\vec{H} \cdot \vec{H}) \\ &\quad \times (\vec{H} \cdot \vec{\rho})\} \cdot \Delta \vec{\rho} = -\frac{1}{\Psi} \nabla_{\rho} W(\vec{H}, \vec{\rho}) \\ &\quad \cdot \nabla_H \bar{W}(\vec{H}, \vec{\rho}) - \frac{1}{\Psi} [\nabla_{\rho} W_{311}(\vec{H} \cdot \vec{H}) \\ &\quad \times (\vec{H} \cdot \vec{\rho})] \cdot [\nabla_H \bar{W}(\vec{H}, \vec{\rho})]. \end{aligned} \quad (68)$$

We mention that the case of piston $W_{600I}^- = W_{600I}^+$ was not verified by real ray tracing.

By performing reverse propagation for a spherical surface (actually done by reversing the surface, the stop, the image, and object planes, and by standard forward ray tracing) we found that

$$\begin{aligned} W_I^{+\text{forward}}(\vec{H}, \vec{\rho}) - W_I^{+\text{reverse}}(\vec{H}, \vec{\rho}) \\ = -\frac{1}{\Psi} \nabla_{\rho} W(\vec{H}, \vec{\rho}) \cdot \nabla_H \bar{W}(\vec{H}, \vec{\rho}) + \Delta \Pi(\vec{H}, \vec{\rho}), \end{aligned} \quad (69)$$

where

$$\begin{aligned} \Delta \Pi(\vec{H}, \vec{\rho}) &= \frac{1}{2} W_{311} \Delta\{u^2\}(\vec{H} \cdot \vec{H})(\vec{\rho} \cdot \vec{\rho})(\vec{H} \cdot \vec{\rho}) \\ &\quad + W_{311} \Delta\{u\bar{u}\}(\vec{H} \cdot \vec{H})(\vec{H} \cdot \vec{\rho})^2 \\ &\quad + \frac{1}{2} W_{311} \Delta\{u\bar{u}\}(\vec{H} \cdot \vec{H})^2(\vec{\rho} \cdot \vec{\rho}) \\ &\quad + \frac{3}{2} W_{311} \Delta\{\bar{u}^2\}(\vec{H} \cdot \vec{H})^2(\vec{H} \cdot \vec{\rho}). \end{aligned} \quad (70)$$

The term $W_I^{+\text{reverse}}(\vec{H}, \vec{\rho})$ is the wavefront aberration on reverse ray tracing through the surface

Table 9. Quantities Used in Calculation of Intrinsic Aberration Coefficients with the Aperture Vector $\vec{\rho}$ at the Exit Pupil

$W_{220P} = -\frac{1}{4} \Psi^2 P$
$W_{240CC}^+ = +\frac{1}{16} \frac{A}{r} \Psi^2 \Delta\{\frac{u}{n}\} + \frac{1}{8} \frac{1}{r} \Psi^2 \Delta\{\frac{u^2}{n}\}$
$+ \frac{1}{4} \frac{v^2}{r^2} W_{220P} + \frac{v}{r} u' W_{220P} - \frac{1}{4} \frac{u}{r} \Psi^2 \Delta\{\frac{u}{n}\}$
$W_{420CC}^+ = \frac{3}{16} \frac{1}{r^3} \Psi^4 \Delta\{\frac{1}{n}\} \frac{1}{A^2} (W_{420CC}^+ = 0 \text{ for } A = 0)$
$W_{331CC}^+ = -2W_{220P} \cdot u' \bar{u}'$
$W_{151CC}^+ = -4W_{040} \cdot u' \bar{u}'$
$W_{242CC}^+ = -2W_{040} \cdot \bar{u}'^2$

and placing the aperture vector at the exit pupil (entrance pupil of the unreversed system). The terms in $\Delta \Pi(\vec{H}, \vec{\rho})$ result from placing the reference sphere center at the actual intersection of the chief ray with the Gaussian image plane as discussed in the extrinsic aberrations section. Thus Eq. (69) shows that by swapping the appropriate paraxial quantities in $W_I^+(\vec{H}, \vec{\rho})$ one can obtain $W_I^-(\vec{H}, \vec{\rho})$ as was done for spherical aberration.

Furthermore, the terms

$$\begin{aligned} \Delta \Xi(\vec{H}, \vec{\rho}) &= \frac{1}{2} W_{311} u'^2 (\vec{H} \cdot \vec{H})(\vec{H} \cdot \vec{\rho})(\vec{\rho} \cdot \vec{\rho}) \\ &\quad + W_{311} u' \bar{u}' (\vec{H} \cdot \vec{H})(\vec{H} \cdot \vec{\rho})^2 \\ &\quad + \frac{1}{2} W_{311} u' \bar{u}' (\vec{H} \cdot \vec{H})^2 (\vec{\rho} \cdot \vec{\rho}) \\ &\quad + \frac{3}{2} W_{311} \bar{u}'^2 (\vec{H} \cdot \vec{H})^2 (\vec{H} \cdot \vec{\rho}) \\ &\quad - \frac{1}{\Psi} [\nabla_{\rho} W_{311}(\vec{H} \cdot \vec{H})(\vec{H} \cdot \vec{\rho})] \cdot [\nabla_H \bar{W}(\vec{H}, \vec{\rho})], \end{aligned} \quad (71)$$

account for the effect of changing the center of the reference sphere from the Gaussian image point to the intersection of the chief ray with the Gaussian image plane.

13. Image and Pupil Coefficient Relationships

To determine the pupil aberration coefficients, data for the chief ray are interchanged with data for the

Table 10. Intrinsic Aberration Coefficients with the Aperture Vector $\vec{\rho}$ at the Exit Pupil^a

$W_{060I}^+ = W_{040} [\frac{1}{2} \frac{v^2}{r^2} - \frac{1}{2} A (\frac{u'}{n} + \frac{u}{n}) + 2 \frac{v}{r} u'] - \frac{8}{\Psi} W_{040} \cdot W_{040} \frac{v}{y}$
$W_{151I}^+ = 6 \frac{A}{A} W_{060I}^+ + W_{131} u'^2 + W_{151CC}^+$
$W_{242I}^+ = 12 (\frac{A}{A})^2 W_{060I}^+ + \frac{7}{2} W_{222} u'^2 - 3 W_{131} u' \bar{u}' + W_{242CC}^+$
$W_{333I}^+ = 8 (\frac{A}{A})^3 W_{060I}^+ + 4 (\frac{A}{A})^2 W_{151CC}^+ + 3 \frac{A}{A} W_{222} u'^2 + 2 \frac{A}{A} W_{242CC}^+ + 2 W_{222} u' \bar{u}'$
$W_{240I}^+ = W_{240CC}^+ + 3 (\frac{A}{A})^2 W_{060I}^+ - 8 \frac{1}{\Psi} \frac{A}{A} W_{040} \cdot W_{220P} + W_{222} u'^2 - W_{131} u' \bar{u}'$
$W_{331I}^+ = 4 \frac{A}{A} W_{240I}^+ + 2 \frac{A}{A} W_{242CC}^+ + \frac{A}{A} W_{220} u'^2 + W_{311} u'^2 + W_{331CC}^+$
$W_{422I}^+ = 4 (\frac{A}{A})^2 W_{240I}^+ + 2 \frac{A}{A} W_{331CC}^+ - 2 W_{222} \bar{u}'^2 - W_{220} \bar{u}'^2 + 2 (\frac{A}{A})^2 W_{220} u'^2 + W_{311} u' \bar{u}' + \frac{1}{2} \frac{A}{A} W_{311} u'^2 + 2 \frac{A}{A} W_{220} u' \bar{u}'$
$W_{420I}^+ = 3 (\frac{A}{A})^4 W_{060I}^+ + 2 (\frac{A}{A})^2 W_{240CC}^+ - 4 (\frac{A}{A})^2 \frac{1}{\Psi} W_{131} \cdot W_{220P} - 2 \frac{A}{A} \frac{1}{\Psi} W_{220P} \cdot W_{220P} + W_{420CC}^+ + \frac{A}{A} W_{331CC}^+ + (\frac{A}{A})^2 W_{220P} u'^2$
$+ \frac{1}{2} \frac{A}{A} W_{311} u'^2 - \frac{1}{2} W_{311} u' \bar{u}' + 2 \frac{A}{A} W_{220P} u' \bar{u}' + (\frac{A}{A})^2 W_{222} u'^2 - \frac{1}{2} W_{222} \bar{u}'^2$
$W_{511I}^+ = 6 (\frac{A}{A})^5 W_{060I}^+ + 4 (\frac{A}{A})^3 [W_{240CC}^+ - 2 \frac{1}{\Psi} W_{131} \cdot W_{220P}] + 2 \frac{A}{A} [W_{420CC}^+ - 2 \frac{A}{A} \frac{1}{\Psi} W_{220P} \cdot W_{220P}] + (\frac{A}{A})^3 W_{222} u'^2 + 2 (\frac{A}{A})^2 W_{311} u'^2$
$- (\frac{A}{A})^2 W_{222} u' \bar{u}' - 2 (\frac{A}{A})^2 W_{220P} u' \bar{u}' - \frac{A}{A} W_{222} \bar{u}'^2 + \frac{1}{2} W_{311} \bar{u}'^2$
$W_{600I}^+ = \bar{W}_{060I}^+$

^aThe reference sphere is at the intersection of the chief ray with the Gaussian image plane.

Table 11. Relationships between Intrinsic Coefficients W^- and W^+ of a Spherical Surface^a

$$\begin{aligned}
 W_{060I}^- &= W_{060I}^+ + \frac{4}{\Psi} W_{040} \cdot \bar{W}_{311} \\
 W_{151I}^- &= W_{151I}^+ + \frac{1}{\Psi} [3W_{131} \cdot \bar{W}_{311} + 8W_{040} \cdot \bar{W}_{220} + 8W_{040} \cdot \bar{W}_{222}] \\
 W_{242I}^- &= W_{242I}^+ + \frac{1}{\Psi} [2W_{222} \cdot \bar{W}_{311} + 4W_{131} \cdot \bar{W}_{220} + 6W_{131} \cdot \bar{W}_{222} + 8W_{040} \cdot \bar{W}_{131}] \\
 W_{333I}^- &= W_{333I}^+ + \frac{1}{\Psi} [4W_{131} \cdot \bar{W}_{131} + 4W_{222} \cdot \bar{W}_{222}] \\
 W_{240I}^- &= W_{240I}^+ + \frac{1}{\Psi} [2W_{220} \cdot \bar{W}_{311} + 2W_{131} \cdot \bar{W}_{220} + 4W_{040} \cdot \bar{W}_{131}] \\
 W_{331I}^- &= W_{331I}^+ + \frac{1}{\Psi} [5W_{131} \cdot \bar{W}_{131} + 4W_{220} \cdot \bar{W}_{222} + 4W_{222} \cdot \bar{W}_{220} + W_{311} \cdot \bar{W}_{311} + 16W_{040} \cdot \bar{W}_{040}] \\
 W_{422I}^- &= W_{422I}^+ + \frac{1}{\Psi} [6W_{222} \cdot \bar{W}_{131} + 8W_{131} \cdot \bar{W}_{040} + 2W_{311} \cdot \bar{W}_{222}] \\
 W_{420I}^- &= W_{420I}^+ + \frac{1}{\Psi} [2W_{220} \cdot \bar{W}_{131} + 4W_{131} \cdot \bar{W}_{040}] \\
 W_{511I}^- &= W_{511I}^+ + \frac{1}{\Psi} [8W_{220} \cdot \bar{W}_{040} + 8W_{222} \cdot \bar{W}_{040}] \\
 W_{600I}^- &= W_{600I}^+
 \end{aligned}$$

^aThe reference sphere is centered at the intersection of the chief ray with the Gaussian image plane.

marginal ray, and then the image coefficients provide the pupil coefficients.

Alternatively, the fourth-order pupil treatment suggests that the sixth-order image and pupil aberrations can be related. That is,

$$\begin{aligned}
 \bar{W}^{(6)}(\vec{H}, \vec{\rho}) + n \cdot S^{(6)}(\vec{H}, \vec{\rho}) &= W^{(6)}(\vec{H}, \vec{\rho}) + n' \\
 &\cdot S'^{(6)}(\vec{H}, \vec{\rho}) + O^{(6)}, \quad (72)
 \end{aligned}$$

where $O^{(6)}$ represents sixth-order terms to be determined.

Table 12 provides the relationships between sixth-order pupil and image coefficients. These were found in analogy with the formula development of this paper and by using real ray tracing to numerically find the magnitude of the coefficients as explained below. The image aberration coefficients depend on the ratio \bar{A}/A , and when the marginal ray is, or is nearly, normal to the spherical surface, $\bar{A} \cong 0$, there can be a singularity in the coefficients W_{240I}^+ , W_{333I}^+ , W_{422I}^+ , W_{420I}^+ , and W_{151I}^+ . It is through the use of the image-pupil relationships that the singularity of computing the coefficients can be avoided.

Note that two forms for \bar{W}_{331I}^+ are given. The form at the bottom of the Table 12 was first obtained from guessing the coefficients with the aid of computer ray tracing. The second form was derived by similarity with the other equations. Both forms match to at least eight decimal places in a computer simulation for several stop and object locations.

Thus the term $O^{(6)}$ in Eq. (72) is given by

$$\begin{aligned}
 O^{(6)} &= \frac{1}{\Psi} \nabla_{\rho} W(\vec{H}, \vec{\rho}) \cdot \nabla_H \bar{W}(\vec{H}, \vec{\rho}) - \Delta \Xi(\vec{H}, \vec{\rho}) \\
 &+ \Delta \bar{\Xi}(\vec{H}, \vec{\rho}), \quad (73)
 \end{aligned}$$

where $\Delta \Xi(\vec{H}, \vec{\rho})$ and $\Delta \bar{\Xi}(\vec{H}, \vec{\rho})$ result from placing the center of the reference sphere at the intersection of the chief ray with the Gaussian image plane and are given by

$$\begin{aligned}
 \Delta \Xi(\vec{H}, \vec{\rho}) &= \frac{1}{2} W_{311} u'^2 (\vec{H} \cdot \vec{H}) (\vec{H} \cdot \vec{\rho}) (\vec{\rho} \cdot \vec{\rho}) \\
 &+ W_{311} u' \bar{u}' (\vec{H} \cdot \vec{H}) (\vec{H} \cdot \vec{\rho})^2 \\
 &+ \frac{1}{2} W_{311} u' \bar{u}' (\vec{H} \cdot \vec{H})^2 (\vec{\rho} \cdot \vec{\rho}) \\
 &+ \frac{3}{2} W_{311} \bar{u}'^2 (\vec{H} \cdot \vec{H})^2 (\vec{H} \cdot \vec{\rho}), \quad (74)
 \end{aligned}$$

$$\begin{aligned}
 \Delta \bar{\Xi}(\vec{H}, \vec{\rho}) &= \frac{1}{2} \bar{W}_{311} u'^2 (\vec{H} \cdot \vec{H}) (\vec{H} \cdot \vec{\rho}) (\vec{\rho} \cdot \vec{\rho}) \\
 &+ \bar{W}_{311} u' \bar{u}' (\vec{H} \cdot \vec{H}) (\vec{H} \cdot \vec{\rho})^2 \\
 &+ \frac{1}{2} \bar{W}_{311} u' \bar{u}' (\vec{H} \cdot \vec{H})^2 (\vec{\rho} \cdot \vec{\rho}) \\
 &+ \frac{3}{2} \bar{W}_{311} \bar{u}'^2 (\vec{H} \cdot \vec{H})^2 (\vec{H} \cdot \vec{\rho}). \quad (75)
 \end{aligned}$$

Table 12. Relationships between Sixth-Order Pupil and Image Aberration Coefficients for a Spherical Surface^a

$$\begin{aligned}
 \bar{W}_{060I}^+ &= W_{600I}^+ \\
 \bar{W}_{151I}^+ &= W_{151I}^+ - \frac{3}{8} \Psi \Delta \{u^4\} + \frac{1}{\Psi} [3W_{311} \cdot \bar{W}_{131} + 8W_{220} \cdot \bar{W}_{040} + 8W_{222} \cdot \bar{W}_{040}] - \frac{3}{2} W_{311} \bar{u}'^2 \\
 \bar{W}_{242I}^+ &= W_{242I}^+ - \frac{3}{4} \Psi \Delta \{u\bar{u}^3\} + \frac{1}{\Psi} [2W_{311} \cdot \bar{W}_{222} + 4W_{220} \cdot \bar{W}_{131} + 6W_{222} \cdot \bar{W}_{131} + 8W_{131} \cdot \bar{W}_{040}] - W_{311} u' \bar{u}' \\
 \bar{W}_{333I}^+ &= W_{333I}^+ - \frac{3}{2} \Psi \Delta \{u^2 \bar{u}^2\} + \frac{1}{\Psi} [4W_{131} \cdot \bar{W}_{131} + 4W_{222} \cdot \bar{W}_{222}] \\
 \bar{W}_{240I}^+ &= W_{240I}^+ - \frac{3}{16} \Psi \Delta \{u\bar{u}^3\} + \frac{1}{\Psi} [2W_{311} \cdot \bar{W}_{220} + 2W_{220} \cdot \bar{W}_{131} + 4W_{131} \cdot \bar{W}_{040}] - \frac{1}{2} W_{311} u' \bar{u}' \\
 \bar{W}_{331I}^+ &= W_{331I}^+ - \frac{12}{16} \Psi \Delta \{u^2 \bar{u}^2\} + \frac{1}{\Psi} [5W_{131} \cdot \bar{W}_{131} + 4W_{220} \cdot \bar{W}_{220} + 4W_{220} \cdot \bar{W}_{222} + 4W_{222} \cdot \bar{W}_{220} + W_{311} \cdot \bar{W}_{311} \\
 &+ 16W_{040} \cdot \bar{W}_{040}] + \frac{1}{2} \bar{W}_{311} \bar{u}'^2 - \frac{1}{2} W_{311} u'^2 \\
 \bar{W}_{422I}^+ &= W_{422I}^+ - \frac{3}{4} \Psi \Delta \{u^3 \bar{u}\} + \frac{1}{\Psi} [2W_{222} \cdot \bar{W}_{311} + 4W_{131} \cdot \bar{W}_{220} + 6W_{131} \cdot \bar{W}_{222} + 8W_{040} \cdot \bar{W}_{131}] + \bar{W}_{311} u' \bar{u}' \\
 \bar{W}_{420I}^+ &= W_{420I}^+ - \frac{3}{16} \Psi \Delta \{u^3 \bar{u}\} + \frac{1}{\Psi} [2W_{220} \cdot \bar{W}_{311} + 2W_{131} \cdot \bar{W}_{220} + 4W_{040} \cdot \bar{W}_{131}] + \frac{1}{2} \bar{W}_{311} u' \bar{u}' \\
 \bar{W}_{511I}^+ &= W_{511I}^+ - \frac{3}{8} \Psi \Delta \{u^4\} + \frac{1}{\Psi} [3W_{131} \cdot \bar{W}_{311} + 8W_{040} \cdot \bar{W}_{220} + 8W_{040} \cdot \bar{W}_{222}] + \frac{3}{2} \bar{W}_{311} u'^2 \\
 \bar{W}_{600I}^+ &= W_{060I}^+ \\
 \bar{W}_{331I}^+ &= W_{331I}^+ - \frac{12}{16} \Psi \Delta \{u^2 \bar{u}^2\} + \frac{1}{\Psi} [5W_{131} \cdot \bar{W}_{131} + 4W_{220} \cdot \bar{W}_{220} + 4W_{220} \cdot \bar{W}_{222} + 4W_{222} \cdot \bar{W}_{220} + W_{311} \cdot \bar{W}_{311} \\
 &+ 16W_{040} \cdot \bar{W}_{040}] + \frac{1}{\Psi} W_{311} [W_{131} - \bar{W}_{311}] + \frac{1}{2} [W_{131} \cdot \bar{u}'^2 - \bar{W}_{131} \cdot u'^2 - W_{222} (u\bar{u} + u'\bar{u}') + \bar{W}_{222} (u\bar{u} + u'\bar{u}')]
 \end{aligned}$$

^aThe reference sphere is centered at the intersection of the chief ray with the Gaussian image plane.

14. Eikonal Function

By noting that except for a piston term and the algebraic sign the function $S_g(\vec{H}, \vec{\rho})$ and the reference sphere function $S'(\vec{H}, \vec{\rho})$ are equal, and using Eq. (19), we can express the eikonal function for a spherical surface with the aperture vector at the exit pupil plane. In this treatment the eikonal function gives the optical path from the object point to the exit pupil plane:

$$E(\vec{H}, \vec{\rho}) = -n' \cdot S'(\vec{H}, \vec{\rho}) - W(\vec{H}, \vec{\rho}), \quad (76)$$

where the zero-order and second-order terms are not accounted for.

The zero-order term of the eikonal is

$$E^{(0)}(\vec{H}, \vec{\rho}) = n \cdot \frac{y}{u} - n' \cdot \frac{\bar{y}}{\bar{u}}, \quad (77)$$

which represents the on-axis optical path from the object to the exit pupil.

The second-order terms of the eikonal are

$$E^{(2)}(\vec{H}, \vec{\rho}) = \frac{1}{2} \Psi \frac{\bar{u}}{u} (\vec{H} \cdot \vec{H}) + \Psi \cdot (\vec{H} \cdot \vec{\rho}) + \frac{1}{2} \Psi \frac{u'}{\bar{u}} (\vec{\rho} \cdot \vec{\rho}). \quad (78)$$

The fourth-order terms of the eikonal are

$$E^{(4)}(\vec{H}, \vec{\rho}) = \frac{1}{8} \Psi \Delta \left(\frac{\bar{u}^3}{u} \right) (\vec{H} \cdot \vec{H})^2 - n' \cdot S'^{(4)}(\vec{H}, \vec{\rho}) - W^{(4)}(\vec{H}, \vec{\rho}), \quad (79)$$

and the sixth-order terms are

$$E^{(6)}(\vec{H}, \vec{\rho}) = -\frac{1}{16} \Psi \Delta \left(\frac{\bar{u}^5}{u} \right) (\vec{H} \cdot \vec{H})^3 - n' \cdot S'^{(6)}(\vec{H}, \vec{\rho}) - W^{+(6)}(\vec{H}, \vec{\rho}). \quad (80)$$

15. Coefficients for a System of Surfaces

Knowledge of the intrinsic and extrinsic coefficients permits us to write the aberration coefficients for a system of j surfaces. These coefficients comprise the sum of all the intrinsic coefficients and the sum of all the extrinsic coefficients as define in Table 5. The coefficients are given in Table 13 for the case of having the aperture vector at the exit pupil. The sums are over the j surfaces as indicated by the summation indices. The right upper indices, i and m , added to the coefficients are to indicate that the coefficient pertains to surface i or m . For $i = 1$ the sums in the curly brackets are defined to be equal to zero.

16. Irradiance Function

In this section we determine the irradiance function $I(\vec{H}, \vec{\rho})$ that gives the beam relative irradiance across the exit pupil for each field point. Since the optical

system has axial symmetry and in analogy with the aberration function the irradiance function can also be expressed as a polynomial, and to sixth order it is

$$\begin{aligned} I(\vec{H}, \vec{\rho}) &= \sum_{j,m,n} I_{k,l,m} (\vec{H} \cdot \vec{H})^j \cdot (\vec{H} \cdot \vec{\rho})^m \cdot (\vec{\rho} \cdot \vec{\rho})^n \\ &= I_{000} + I_{200} (\vec{H} \cdot \vec{H}) + I_{111} (\vec{H} \cdot \vec{\rho}) + I_{020} (\vec{\rho} \cdot \vec{\rho}) \\ &\quad + I_{040} (\vec{\rho} \cdot \vec{\rho})^2 + I_{131} (\vec{H} \cdot \vec{\rho}) (\vec{\rho} \cdot \vec{\rho}) + I_{222} (\vec{H} \cdot \vec{\rho})^2 \\ &\quad + I_{220} (\vec{H} \cdot \vec{H}) (\vec{\rho} \cdot \vec{\rho}) + I_{311} (\vec{H} \cdot \vec{H}) (\vec{H} \cdot \vec{\rho}) \\ &\quad + I_{400} (\vec{H} \cdot \vec{H})^2 + I_{240} (\vec{H} \cdot \vec{H}) (\vec{\rho} \cdot \vec{\rho})^2 \\ &\quad + I_{331} (\vec{H} \cdot \vec{H}) (\vec{H} \cdot \vec{\rho}) (\vec{\rho} \cdot \vec{\rho}) + I_{422} (\vec{H} \cdot \vec{H}) (\vec{H} \cdot \vec{\rho})^2 \\ &\quad + I_{420} (\vec{H} \cdot \vec{H})^2 (\vec{\rho} \cdot \vec{\rho}) + I_{511} (\vec{H} \cdot \vec{H})^2 (\vec{H} \cdot \vec{\rho}) \\ &\quad + I_{600} (\vec{H} \cdot \vec{H})^3 + I_{060} (\vec{\rho} \cdot \vec{\rho})^3 + I_{151} (\vec{H} \cdot \vec{\rho}) (\vec{\rho} \cdot \vec{\rho})^2 \\ &\quad + I_{242} (\vec{H} \cdot \vec{\rho})^2 (\vec{\rho} \cdot \vec{\rho}) + I_{333} (\vec{H} \cdot \vec{\rho})^3. \end{aligned} \quad (81)$$

The terms in the irradiance function represent variations, or apodization aberrations, in the irradiance of the optical beams at the exit pupil. These variations are also arranged according to the algebraic order of the terms. We wish to determine the irradiance function coefficients $I_{k,l,m}$. For this we will locate the aperture vector at the exit pupil. Given that the optical power through the system must be conserved, we must conserve the flux and satisfy

$$\begin{aligned} I_0 \cdot I(\vec{H}, \vec{\rho} + \Delta \vec{\rho}) \cdot d^2 S &= I_0 \cdot I(\vec{H}, \vec{\rho} + \Delta \vec{\rho}) \cdot d^2 S' \cdot J(\vec{H}, \vec{\rho}) \\ &= I'_0 \cdot I'(\vec{H}, \vec{\rho}) \cdot d^2 S', \end{aligned} \quad (82)$$

where $I(\vec{H}, \vec{\rho})$ is the irradiance function at the entrance pupil plane of the system, $I'(\vec{H}, \vec{\rho})$ is the irradiance function at the exit pupil plane, $d^2 S$ is the element of area at the entrance pupil, $d^2 S'$ is the element of area at the exit pupil, and $J(\vec{H}, \vec{\rho})$ is the Jacobian determinant.

Because of the presence of pupil aberrations Eq. (82) determines the irradiance function $I(\vec{H}, \vec{\rho} + \Delta \vec{\rho})$ at point $\vec{\rho} + \Delta \vec{\rho}$ of the entrance pupil. The Jacobian determinant provides the relationship between the area elements at the pupil planes, and to conserve the flux within Gaussian optics we have $I_0 \cdot y_{\text{pupil}}^2 = I'_0 \cdot y_{\text{pupil}}'^2$.

Let \vec{g} be a unit vector in the direction of $\vec{\rho}$, \vec{h} be a unit vector in the direction of \vec{H} , and \vec{i} be a unit vector perpendicular to \vec{h} . The displacement vector $\Delta \vec{\rho} = \Delta \vec{\rho}_g + \Delta \vec{\rho}_h$ has two components, one in the direction $\vec{\rho}$ and the other in the direction of \vec{h} . To obtain the Jacobian determinant we express the displacement vector $\Delta \vec{\rho}$ in orthogonal coordinates along \vec{h} and \vec{i} as $\Delta \vec{\rho} = \Delta \rho_i \vec{i} + \Delta \rho_h \vec{h} = (\Delta \vec{\rho}_g \cdot \vec{i}) \vec{i} + (\Delta \vec{\rho}_g \cdot \vec{h} + \Delta \vec{\rho}_h \cdot \vec{h}) \vec{h}$. Then, with $\rho'_h = \rho_h + \Delta \rho_h$, $\rho'_i = \rho_i + \Delta \rho_i$ giving the position of a giving ray at the entrance pupil, we have that the Jacobian determinant is

Table 13. Sixth-Order Aberration Coefficients for a System of j Surfaces

$$\begin{aligned}
 W_{060}^+ &= \sum_{i=1}^j W_{060I}^{+i} - \frac{1}{\Psi} \sum_{i=1}^j \{ \bar{W}_{311}^i \sum_{m=1}^{i-1} 4W_{040}^m \} \\
 W_{151}^+ &= \sum_{i=1}^j W_{151I}^{+i} - \frac{1}{\Psi} \sum_{i=1}^j \{ \bar{W}_{311}^i \sum_{m=1}^{i-1} 3W_{131}^m \} - \frac{1}{\Psi} \sum_{i=1}^j \{ \bar{W}_{220}^i \sum_{m=1}^{i-1} 8W_{040}^m \} - \frac{1}{\Psi} \sum_{i=1}^j \{ \bar{W}_{222}^i \sum_{m=1}^{i-1} 8W_{040}^m \} \\
 W_{242}^+ &= \sum_{i=1}^j W_{242I}^{+i} - \frac{1}{\Psi} \sum_{i=1}^j \{ \bar{W}_{311}^i \sum_{m=1}^{i-1} 2W_{222}^m \} - \frac{1}{\Psi} \sum_{i=1}^j \{ \bar{W}_{220}^i \sum_{m=1}^{i-1} 4W_{131}^m \} - \frac{1}{\Psi} \sum_{i=1}^j \{ \bar{W}_{222}^i \sum_{m=1}^{i-1} 6W_{131}^m \} - \frac{1}{\Psi} \sum_{i=1}^j \{ \bar{W}_{131}^i \sum_{m=1}^{i-1} 8W_{040}^m \} \\
 W_{333}^+ &= \sum_{i=1}^j W_{333I}^{+i} - \frac{1}{\Psi} \sum_{i=1}^j \{ \bar{W}_{131}^i \sum_{m=1}^{i-1} 4W_{131}^m \} - \frac{1}{\Psi} \sum_{i=1}^j \{ \bar{W}_{222}^i \sum_{m=1}^{i-1} 4W_{222}^m \} \\
 W_{240}^+ &= \sum_{i=1}^j W_{240I}^{+i} - \frac{1}{\Psi} \sum_{i=1}^j \{ \bar{W}_{220}^i \sum_{m=1}^{i-1} 2W_{131}^m \} - \frac{1}{\Psi} \sum_{i=1}^j \{ \bar{W}_{311}^i \sum_{m=1}^{i-1} 2W_{220}^m \} - \frac{1}{\Psi} \sum_{i=1}^j \{ \bar{W}_{131}^i \sum_{m=1}^{i-1} 4W_{040}^m \} \\
 W_{331}^+ &= \sum_{i=1}^j W_{331I}^{+i} - \frac{1}{\Psi} \sum_{i=1}^j \{ \bar{W}_{131}^i \sum_{m=1}^{i-1} 5W_{131}^m \} - \frac{1}{\Psi} \sum_{i=1}^j \{ \bar{W}_{220}^i \sum_{m=1}^{i-1} 4W_{220}^m \} - \frac{1}{\Psi} \sum_{i=1}^j \{ \bar{W}_{222}^i \sum_{m=1}^{i-1} 4W_{220}^m \} - \frac{1}{\Psi} \sum_{i=1}^j \{ \bar{W}_{220}^i \sum_{m=1}^{i-1} 4W_{222}^m \} \\
 &\quad - \frac{1}{\Psi} \sum_{i=1}^j \{ \bar{W}_{311}^i \sum_{m=1}^{i-1} W_{311}^m \} - \frac{1}{\Psi} \sum_{i=1}^j \{ \bar{W}_{040}^i \sum_{m=1}^{i-1} 16W_{040}^m \} + \sum_{i=1}^j \{ \frac{1}{2} \Delta^i \{ u^2 \} \sum_{m=1}^{i-1} W_{311}^m \} \\
 W_{422}^+ &= \sum_{i=1}^j W_{422I}^{+i} - \frac{1}{\Psi} \sum_{i=1}^j \{ \bar{W}_{222}^i \sum_{m=1}^{i-1} 2W_{311}^m \} - \frac{1}{\Psi} \sum_{i=1}^j \{ \bar{W}_{131}^i \sum_{m=1}^{i-1} 4W_{220}^m \} - \frac{1}{\Psi} \sum_{i=1}^j \{ \bar{W}_{131}^i \sum_{m=1}^{i-1} 6W_{222}^m \} - \frac{1}{\Psi} \sum_{i=1}^j \{ \bar{W}_{040}^i \sum_{m=1}^{i-1} 8W_{131}^m \} \\
 &\quad + \sum_{i=1}^j \{ \Delta^i \{ u\bar{u} \} \sum_{m=1}^{i-1} W_{311}^m \} \\
 W_{420}^+ &= \sum_{i=1}^j W_{420I}^{+i} - \frac{1}{\Psi} \sum_{i=1}^j \{ \bar{W}_{131}^i \sum_{m=1}^{i-1} 2W_{220}^m \} - \frac{1}{\Psi} \sum_{i=1}^j \{ \bar{W}_{220}^i \sum_{m=1}^{i-1} 2W_{311}^m \} - \frac{1}{\Psi} \sum_{i=1}^j \{ \bar{W}_{040}^i \sum_{m=1}^{i-1} 4W_{131}^m \} + \sum_{i=1}^j \{ \frac{1}{2} \Delta^i \{ u\bar{u} \} \sum_{m=1}^{i-1} W_{311}^m \} \\
 W_{511}^+ &= \sum_{i=1}^j W_{511I}^{+i} - \frac{1}{\Psi} \sum_{i=1}^j \{ \bar{W}_{131}^i \sum_{m=1}^{i-1} 3W_{311}^m \} - \frac{1}{\Psi} \sum_{i=1}^j \{ \bar{W}_{040}^i \sum_{m=1}^{i-1} 8W_{220}^m \} - \frac{1}{\Psi} \sum_{i=1}^j \{ \bar{W}_{040}^i \sum_{m=1}^{i-1} 8W_{222}^m \} + \sum_{i=1}^j \{ \frac{3}{2} \Delta^i \{ \bar{u}^2 \} \sum_{m=1}^{i-1} W_{311}^m \} \\
 W_{600}^+ &= \sum_{i=1}^j W_{600I}^{+i} - \frac{1}{\Psi} \sum_{i=1}^j \{ \bar{W}_{040}^i \sum_{m=1}^{i-1} 4W_{311}^m \}
 \end{aligned}$$

$$\begin{aligned}
 J(\vec{H}, \vec{\rho}) &= \frac{y_{\text{pupil}}^2}{y_{\text{pupil}}'^2} \cdot \left\{ 1 + \frac{\partial \Delta \rho_h}{\partial \rho_h} + \frac{\partial \Delta \rho_i}{\partial \rho_i} \right. \\
 &\quad \left. + \frac{\partial \Delta \rho_h}{\partial \rho_h} \frac{\partial \Delta \rho_i}{\partial \rho_i} - \frac{\partial \Delta \rho_i}{\partial \rho_h} \frac{\partial \Delta \rho_h}{\partial \rho_i} \right\}. \quad (83)
 \end{aligned}$$

Since $\rho_h = \vec{\rho} \cdot \vec{h} = \rho \cdot \cos(\phi)$ and $\rho_i = \vec{\rho} \cdot \vec{i} = \rho \cdot \sin(\phi)$, we can write for the partial derivatives

$$\frac{\partial \Delta \rho_h}{\partial \rho_h} = \frac{\partial \Delta \rho_h}{\partial \rho} \frac{\partial \rho}{\partial \rho_h} = \frac{1}{\cos(\phi)} \frac{\partial \Delta \rho_h}{\partial \rho}, \quad (84)$$

$$\frac{\partial \Delta \rho_i}{\partial \rho_i} = \frac{\partial \Delta \rho_i}{\partial \rho} \frac{\partial \rho}{\partial \rho_i} = \frac{1}{\sin(\phi)} \frac{\partial \Delta \rho_i}{\partial \rho}, \quad (85)$$

$$\frac{\partial \Delta \rho_h}{\partial \rho_i} = \frac{\partial \Delta \rho_h}{\partial \rho} \frac{\partial \rho}{\partial \rho_i} = \frac{1}{\sin(\phi)} \frac{\partial \Delta \rho_h}{\partial \rho}, \quad (86)$$

$$\frac{\partial \Delta \rho_i}{\partial \rho_h} = \frac{\partial \Delta \rho_i}{\partial \rho} \frac{\partial \rho}{\partial \rho_h} = \frac{1}{\cos(\phi)} \frac{\partial \Delta \rho_i}{\partial \rho}, \quad (87)$$

and the Jacobian determinant simplifies to

$$\begin{aligned}
 J(\vec{H}, \vec{\rho}) &= \frac{y_{\text{pupil}}^2}{y_{\text{pupil}}'^2} \cdot \left\{ 1 + \frac{\partial \Delta \rho_h}{\partial \rho_h} + \frac{\partial \Delta \rho_i}{\partial \rho_i} \right\} \\
 &= \frac{y_{\text{pupil}}^2}{y_{\text{pupil}}'^2} \cdot \{ 1 + \nabla_{\rho} \Delta \vec{\rho} \}, \quad (88)
 \end{aligned}$$

where $\nabla_{\rho} \Delta \vec{\rho}$ stands for the divergence of $\Delta \vec{\rho}$. To the fourth order of approximation we can write

$$I(\vec{H}, \vec{\rho} + \Delta \vec{\rho}) - I(\vec{H}, \vec{\rho}) \cong \nabla_{\rho} I(\vec{H}, \vec{\rho}) \cdot \Delta \vec{\rho} \quad (89)$$

and recast Eq. (82) as

$$I'(\vec{H}, \vec{\rho}) \cong [\nabla_{\rho} I(\vec{H}, \vec{\rho}) \cdot \Delta \vec{\rho} + I(\vec{H}, \vec{\rho})] (1 + \nabla_{\rho} \Delta \vec{\rho}). \quad (90)$$

Equation (90) relates the irradiance at the exit pupil to the irradiance at the entrance pupil through the entrance pupil displacement vector $\Delta \vec{\rho}$. It is valid to the fourth order of approximation in the field and aperture variables, as the error in Eq. (89) is of sixth order.

Furthermore, since the displacement vector $\Delta \vec{\rho}$ is given to third-order by

$$\Delta \vec{\rho} = \Delta \vec{\rho}_g + \Delta \vec{\rho}_h = -\frac{1}{\Psi} \nabla_H \bar{W}(\vec{H}, \vec{\rho}), \quad (91)$$

we can recast Eq. (90) as

$$\begin{aligned}
 I'(\vec{H}, \vec{\rho}) - I(\vec{H}, \vec{\rho}) &\cong -\frac{1}{\Psi} \nabla_{\rho} I(\vec{H}, \vec{\rho}) \nabla_H \bar{W}(\vec{H}, \vec{\rho}) \\
 &\quad - \frac{1}{\Psi} I(\vec{H}, \vec{\rho}) \nabla_{\rho} \nabla_H \bar{W}(\vec{H}, \vec{\rho}), \quad (92)
 \end{aligned}$$

where we have neglected terms higher than fourth order and where $\nabla_{\rho} \nabla_H \bar{W}(\vec{H}, \vec{\rho})$ stands for the divergence with respect to ρ of the gradient with respect to \vec{H} of the pupil aberration function $\bar{W}(\vec{H}, \vec{\rho})$. Equation (92) requires the irradiance $I(\vec{H}, \vec{\rho})$ at the entrance pupil and the pupil aberration function $\bar{W}(\vec{H}, \vec{\rho})$. This equation permits finding terms of the irradiance function $I'(\vec{H}, \vec{\rho})$ at the exit pupil. The equation is valid to the second order of approximation in the field and aperture variables. However, if there are no sixth-order pupil aberrations, or if the displacement vector $\Delta \vec{\rho}$ is made to account for up to fifth-order transverse ray errors at the entrance pupil, then Eq. (92) would be valid to the fourth-order of approximation.

The calculation of the divergence and gradient turns out to be simplified. Thompson [2] has shown that the gradient operator is simply given by the derivative of the function with respect to the designated vector; for example,

$$\begin{aligned}\nabla_{\rho} W(\vec{H}, \vec{\rho}) &= \left(\frac{\partial}{\partial \rho_h} W(\vec{H}, \vec{\rho}) \right) \vec{h} + \left(\frac{\partial}{\partial \rho_i} W(\vec{H}, \vec{\rho}) \right) \vec{i} \\ &= \frac{\partial}{\partial \vec{\rho}} W(\vec{H}, \vec{\rho}).\end{aligned}\quad (93)$$

The reasoning can be extended to show that the divergence becomes the derivative with respect to the designated vector; this is

$$\begin{aligned}\nabla_{\rho} (\nabla_H \bar{W}(\vec{H}, \vec{\rho})) &= \frac{\partial}{\partial \rho_h} (\nabla_H \bar{W}(\vec{H}, \vec{\rho}) \cdot \vec{h}) \\ &\quad + \frac{\partial}{\partial \rho_i} (\nabla_H \bar{W}(\vec{H}, \vec{\rho}) \cdot \vec{i}) \\ &= \frac{\partial}{\partial \vec{\rho}} \frac{\partial}{\partial \vec{H}} W(\vec{H}, \vec{\rho}).\end{aligned}\quad (94)$$

In this process we are taking the derivative with respect to a vector. This gives a vector in the case of a scalar (build up from vectors), and a scalar in the case of a vector.

The zero-order terms for both irradiance functions at the entrance and exit pupils are equal to one. With no second-order terms in the aberration function, the terms $\nabla_{\rho} I(\vec{H}, \vec{\rho}) \nabla_H \bar{W}(\vec{H}, \vec{\rho})$ result in other terms that are at least of fourth order. The zero- and second-order terms of the irradiance function in terms of pupil aberrations are given in Table 14.

The second-order term $I'_{020}(\vec{\rho} \cdot \vec{\rho})$ represents a parabolic apodization for all the field beams. The term $I'_{111}(\vec{H} \cdot \vec{\rho})$ represents a linear apodization as a function of either the aperture or the field of view. The term $I'_{200}(\vec{H} \cdot \vec{H})$ represents a quadratic irradiance change as a function of the field of view; this is known as the Slyusarev effect.

17. Irradiance Transport Equation

In this section we show that Eq. (92) can be rewritten as an irradiance transport equation. In free space we have $\Delta \Omega = 0$, and the relationship between the gradient of the aberration function and the gradient of the pupil aberration function is

$$\nabla_H \bar{W}(\vec{H}, \vec{\rho}) = \frac{\bar{y}_{PP}}{y_{PP}} \nabla_{\rho} W(\vec{H}, \vec{\rho}).\quad (95)$$

Then we can rewrite Eq. (92) for the change of irradiance between two planes, here the rear principal plane and the exit pupil plane, as

$$\begin{aligned}\Delta I(\vec{H}, \vec{\rho}) &= I'(\vec{H}, \vec{\rho}) - I(\vec{H}, \vec{\rho}) \\ &\cong -\frac{1}{\Psi} \frac{\bar{y}_{PP}}{y_{PP}} \nabla_{\rho} I(\vec{H}, \vec{\rho}) \cdot \nabla_{\rho} W(\vec{H}, \vec{\rho}) \\ &\quad - \frac{1}{\Psi} \frac{\bar{y}_{PP}}{y_{PP}} I(\vec{H}, \vec{\rho}) \nabla_{\rho}^2 W(\vec{H}, \vec{\rho}),\end{aligned}\quad (96)$$

where $\nabla_{\rho}^2 W(\vec{H}, \vec{\rho})$ stands for the Laplacian of the aberration function,

$$\begin{aligned}\nabla_{\rho}^2 W(\vec{H}, \vec{\rho}) &= \frac{\partial^2 W(\vec{H}, \vec{\rho})}{\partial \rho_h^2} + \frac{\partial^2 W(\vec{H}, \vec{\rho})}{\partial \rho_i^2} \\ &= \frac{\partial}{\partial \vec{\rho}} \left(\frac{\partial}{\partial \vec{\rho}} W(\vec{H}, \vec{\rho}) \right).\end{aligned}\quad (97)$$

Since

$$\frac{\bar{y}_{PP}}{y_{PP}} = -\frac{\Delta Z}{(l - \Delta Z) y_{PP}} \bar{y}_{\text{image}} = -\frac{\Psi}{n} \frac{\Delta Z}{y_{PP} \cdot y_{\text{pupil}}},$$

Eq. (96) becomes

$$\begin{aligned}\frac{\Delta I(\vec{H}, \vec{\rho})}{\Delta Z} &\cong \frac{1}{n \cdot y_{PP} \cdot y_{\text{pupil}}} (\nabla_{\rho} I(\vec{H}, \vec{\rho}) \cdot \nabla_{\rho} W(\vec{H}, \vec{\rho}) \\ &\quad + I(\vec{H}, \vec{\rho}) \cdot \nabla_{\rho}^2 W(\vec{H}, \vec{\rho})).\end{aligned}\quad (98)$$

For very small propagation distances ΔZ we have that $n \cdot y_{PP} \cdot y_{\text{pupil}}$ becomes $n \cdot y_{PP} \cdot y_{PP}$, $\Delta I(\vec{H}, \vec{\rho}) / \Delta Z$ becomes $\partial I(\vec{H}, \vec{\rho}) / \partial Z$, and we can write the equation as

$$\begin{aligned}\frac{\partial I(\vec{H}, \vec{\rho})}{\partial Z} &\cong \frac{1}{n \cdot y_{PP} \cdot y_{PP}} [\nabla_{\rho} I(\vec{H}, \vec{\rho}) \cdot \nabla_{\rho} W(\vec{H}, \vec{\rho}) \\ &\quad + I(\vec{H}, \vec{\rho}) \nabla_{\rho}^2 W(\vec{H}, \vec{\rho})],\end{aligned}\quad (99)$$

which is equivalent to irradiance transport equation (9),

$$\begin{aligned}\frac{\partial I(X, Y)}{\partial Z} &= -[\nabla I(X, Y) \cdot \nabla \Phi(X, Y) \\ &\quad + I(X, Y) \nabla^2 \Phi(X, Y)],\end{aligned}\quad (100)$$

where the function $\Phi(X, Y)$ represents the optical phase. This development reveals that the term $\nabla I(X, Y) \cdot \nabla \Phi(X, Y)$ in Eq. (100) can be interpreted as accounting for the effects of coordinate distortion. The term $I(X, Y) \nabla^2 \Phi(X, Y)$ results from the Jacobian determinant that relates the elements of the area, d^2S and d^2S' .

Equation (98) is a generalized irradiance transport equation that is not limited to small propagation distances. It is written in terms of normalized field and aperture vectors and not in terms of absolute coordinates. The product of the marginal ray height at the principal plane and at the exit pupil accounts for the change of absolute to normalized coordinates.

Table 14. Zero- and Second-Order Terms of the Irradiance Function

I'_{000}	$= 1$
$I'_{020}(\vec{\rho} \cdot \vec{\rho})$	$= -\frac{3}{\Psi} \bar{W}_{311}(\vec{\rho} \cdot \vec{\rho})$
$I'_{111}(\vec{H} \cdot \vec{\rho})$	$= -[\frac{4}{\Psi} \bar{W}_{220} + \frac{6}{\Psi} \bar{W}_{222}](\vec{H} \cdot \vec{\rho})$
$I'_{200}(\vec{H} \cdot \vec{H})$	$= -\frac{6}{\Psi} \bar{W}_{131}(\vec{H} \cdot \vec{H})$

Equations (92) and (98) assume that no second-order terms are present in the aberration function, as their effect on the irradiance is already accounted for by $I_0 \cdot y_{\text{pupil}}^2 = I'_0 \cdot y'^2_{\text{pupil}}$. The use of normalized coordinates permits Eq. (98) to work for large propagation distances; however, this equation is not valid for calculating irradiance changes near or at a ray caustic. The wavefronts are assumed to be smooth as described by the aberration function and unclipped by an aperture so that edge diffraction or multiple beam interference does not take place. The irradiance equations and the propagation equations discussed above describe the geometric wavefront and irradiance changes when an ensemble of wavefronts travels some distance. Effectively, we are propagating the wavefront to sixth order and the irradiance to fourth order in the field and aperture variables (here we assume that $\Delta \vec{\rho}$ accounts for up to fifth-order transverse ray errors).

For the case of having uniform irradiance at the initial plane $I(\vec{H}, \vec{\rho}) = 1$ we have that $\nabla_{\rho} I(\vec{H}, \vec{\rho}) = 0$, and in the presence of spherical aberration $W_{040}(\vec{\rho} \cdot \vec{\rho})^2$ we have that Eq. (98) reduces to

$$\begin{aligned} \frac{\Delta I(\vec{H}, \vec{\rho})}{\Delta Z} &\cong \frac{1}{n \cdot y_{PP} \cdot y_{\text{pupil}}} \nabla_{\rho}^2 W(\vec{H}, \vec{\rho}) \\ &= \frac{1}{n \cdot y_{PP} \cdot y_{\text{pupil}}} 12W_{040}(\vec{\rho} \cdot \vec{\rho}). \end{aligned} \quad (101)$$

With positive spherical aberration the wavefront leads the reference sphere in propagating from left to right a distance ΔZ . Then the irradiance increases on propagation, and the algebraic sign in Eq. (99) is correct. From pupil theory and for a spherical surface we have $4W_{040} \frac{\bar{y}}{y} = \bar{W}_{311} - \bar{W}_{311}^0$. For a flat surface $\Delta \bar{\Omega} = 0$, $\bar{W}_{311}^0 = 0$, $4W_{040} \frac{\bar{y}}{y} = \bar{W}_{311}$, and it follows that

$$\begin{aligned} \Delta I(\vec{H}, \vec{\rho}) &\cong \frac{\Delta Z}{n \cdot \bar{y}_{PP} \cdot y_{\text{pupil}}} 3\bar{W}_{311}(\vec{\rho} \cdot \vec{\rho}) \\ &= -\frac{3}{\bar{\Psi}} \bar{W}_{311}(\vec{\rho} \cdot \vec{\rho}), \end{aligned} \quad (102)$$

in agreement with Table 14. The positive spherical aberration leads to barrel distortion of the exit pupil. The ratio d^2S'/d^2S of the elements of the area decreases and the irradiance at the exit pupil increases to conserve the flux. The difference in algebraic sign between Eq. (99) and irradiance transport equation (100) is due to the difference in sign between the wave aberration function $W(\vec{H}, \vec{\rho})$ and the phase function $\Phi(X, Y)$ used in describing the optical field.

18. Coefficient Verification

To find the algebraic form of the aberration coefficients it was indispensable to know their magnitude. A computer program was written to numerically determine the coefficients by making an iterative fit to a selected set of optical path difference points across the aperture and field of view of an optical system.

For example, for spherical aberration the following iterative loop was executed:

```

FOR j = 1 to 100
  ρ = 0.2
  OPD = OPD(ρ)
  W020 = [OPD - W040ρ4 - W060ρ6 - W080ρ8 - W0100ρ10] · ρ-2
  ρ = 0.4
  OPD = OPD(ρ)
  W040 = [OPD - W020ρ2 - W060ρ6 - W080ρ8 - W0100ρ10] · ρ-4
  ρ = 0.6
  OPD = OPD(ρ)
  W060 = [OPD - W020ρ2 - W040ρ4 - W080ρ8 - W0100ρ10] · ρ-6
  ρ = 0.8
  OPD = OPD(ρ)
  W080 = [OPD - W020ρ2 - W040ρ4 - W060ρ6 - W0100ρ10] · ρ-8
  ρ = 1
  OPD = OPD(ρ)
  W0100 = [OPD - W020ρ2 - W040ρ4 - W060ρ6 - W080ρ8] · ρ-10
NEXT

```

The quantity $OPD = OPD(\rho)$ is the optical path difference at the specified pupil height and with the reference sphere centered at the intersection of the actual chief ray with the Gaussian image plane. After a few iterations of this loop the coefficients converged to the theoretical values with insignificant error for W_{020} , W_{040} , and W_{060} . Similar loops were written to find the remaining aberration coefficients. Tests were done to check the coefficient scalability with respect to field and aperture. Coincidence of the four-order terms with the Seidel coefficients also helped to verify the coefficients obtained by the fit. For the case of distortion the magnitude of the coefficients W_{311} and W_{511} was found by making an iterative fit to the transverse error $\bar{y}_{\text{image}} \cdot \Delta \vec{H}'$ of the chief ray and using $\Delta \vec{H}' = -\Psi^{-1} \cdot \nabla_{\rho} (W_{311}(\vec{H} \cdot \vec{H})(\vec{H} \cdot \vec{\rho}) + W_{511}(\vec{H} \cdot \vec{H})^2(\vec{H} \cdot \vec{\rho}) + W_{711}(\vec{H} \cdot \vec{H})^3(\vec{H} \cdot \vec{\rho}) + \dots)$. This iterative fit methodology proved to be effective, and the success is due in part to the fact that it was applied to find aberration coefficients of a single surface or of systems with few spherical surfaces. As the number of surfaces increased, the ability of the iterative algorithm to find the correct coefficients significantly decreased.

With the ability to find the magnitude of the coefficients, simple algebraic terms were written to guess some missing terms in the aberration coefficient formulas resulting from shifting the pupil from the center of curvature. Tests of the terms were done with $A = 0$, $\bar{A} = 0$, $y = 0$, $\bar{y} = 0$, $r = \infty$, $u = 0$, $\bar{u} = 0$, and $\Delta(u/n) = 0$. Several conjugate distances and stop positions were also tested for a single surface and for a system of several surfaces. Unless the correct formula was obtained there would not be agreement with the coefficients found with the above iterative loop. With the correct formulas there was an obvious agreement of the coefficients.

19. Self-Consistent Verification

Table 12 gives the pupil aberration coefficients by using the image aberration coefficients, terms of the sphere function, and products of the fourth-order

coefficients. The pupil aberration coefficients can also be found by swapping the chief and marginal ray data in the image aberration coefficients and in the Lagrange invariant. When this is done, the pupil aberration coefficients computed in both manners match. This represents a self-consistent verification. Table 15 presents a comparison of coefficients calculated both ways, where some the differences are in the 15th decimal place and are likely due to the computational approach used. The essentially equality of the coefficients supports the correctness of the aberration coefficients.

20. Aspheric Triplet Lens Example

In this section we provide an example triplet lens that is corrected for all fourth-order and sixth-order aberrations to the 10^{-14} level or better. Four surfaces are aspheric with fourth and sixth-order coefficients of deformation. The contributions from an aspheric surface to the aberration coefficients are derived and given in Appendix B. The design is shown in Fig. 7, and it evolved from a design from Shafer [9]. We reoptimized the lens to reduce the wave aberration residuals from the 10^{-6} level to the 10^{-14} level to critically test the coefficients in this paper. The specifications of the reoptimized triplet are given in Appendix E.

The final values of the wave aberration coefficients are shown in Table 16. For comparison, the fifth-order coefficients from Rimmer's thesis [10] were computed and are also given in Table 16. These two sets of coefficients are nearly zero to the 10^{-14} level or better. Thus, for this triplet lens and in the absence of fourth-order aberrations there is agreement, in that there is no aberration, between the sixth-order theory in this paper and the fifth-order theory of Buchdahl [11]. We point out that Buchdahl's theory provides the fifth-order transverse ray aberration coefficients with the aperture vector at the entrance pupil. Relationships between the Buchdahl coefficients and the wave coefficients in this paper can be established by first describing the Buchdahl coefficients with the aperture vector at the exit pupil. Then the normalized (by the image height) transverse ray aberrations to fifth order are given by

$$\Delta \vec{H}' = -\frac{1}{\cos^3(\theta')} \frac{1}{\Psi} \nabla_{\rho} W(\vec{H}, \vec{\rho}) + O^{(7)}, \quad (103)$$

Table 15. Coefficient Comparison for an Aspheric Surface^a

W_{151}	-0.4193360087176732	-0.4193360087176732
W_{242}	1.3879576582604869	1.3879576582604876
W_{333}	-1.3737719852861099	-1.3737719852861099
W_{240}	0.1318037474153832	0.1318037474153833
W_{331}	-1.5376298938401587	-1.5376298938401600
W_{422}	0.4115466232465593	0.4115466232465597
W_{420}	2.3841052150066186	2.3841052150066186
W_{511}	-2.2205687849607498	-2.2205687849607463

^aThe coefficients are in waves at 586.7 nm.

where

$$\cos(\theta') \cong 1 - \frac{1}{2}(u'^2(\vec{\rho} \cdot \vec{\rho}) + 2u'\bar{u}'(\vec{H} \cdot \vec{\rho}) + \bar{u}'^2(\vec{H} \cdot \vec{H})) \quad (104)$$

and θ' is the angle of a given ray in image space with the optical axis.

The relationships between the fifth-order transverse ray coefficients of Buchdahl and the sixth-order wave coefficients in this paper will be the subject of future work. We point out that in the absence of fourth-order aberrations the Buchdahl coefficients are given by the gradient of the aberration function (sixth-order terms) divided by $n'u'$.

21. Summary

This paper develops a sixth-order theory of wave aberrations for axially symmetric systems. Specific formulas for the sixth-order extrinsic and intrinsic wave aberration coefficients are given, as well as relations between pupil and image aberrations. The paper develops equations for the wavefront propagation to sixth-order of approximation; the equation for free-space propagation in terms of normalized quantities is novel and is not limited to small propagation distances. The concept of the irradiance function is developed, and the second-order irradiance coefficients are found via conservation of flux at the pupils of the optical system and in terms of pupil aberrations. As a result we derived, from purely geometrical considerations, a generalized irradiance transport equation that describes irradiance changes in an optical system. We effectively have provided a solution to the irradiance transport problem in terms of the aberrations of an optical system. Both the wavefront propagation and the irradiance transport equation account for geometric effects and do not consider edge diffraction effects, and unclipped and unfolded beams are assumed. We found it indispensable to verify the formulas for the aberration coefficients with the results from real ray tracing.

The aberration coefficients provided are with the center of the reference sphere at the intersection of the real chief ray with the Gaussian image plane; they describe to sixth order the actual wavefronts computed by optical design software. However, we have indicated the terms that correspond to the case of having the center of the reference sphere at the Gaussian image point. In this latter case the connections between coefficients acquire an elegant mathematical form. We also have shown in terms of the sphere function, the aberration function, and the pupil function the relationship with the eikonal function and have provided specific formulas for the eikonal's expansion coefficients.

Further work could be done to obtain the fourth-order coefficients of the irradiance function and to provide formulas to convert the aberration coefficients to other coordinate systems of interest. However, modern optical design relies significantly

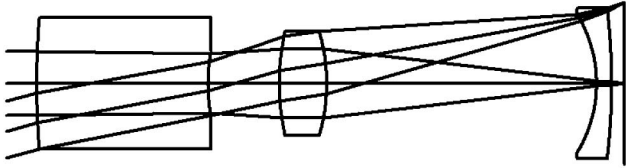


Fig. 7. Aspheric triplet lens corrected for fourth- and sixth-order aberrations to the 10^{-14} wave level.

on real ray tracing and on the insights of aberration theory. This paper gives insight into aberration generation and light propagation in an optical system because it makes visible the underlying structure of how the wavefront deforms as it propagates in an optical system and provides specific formulae. Overall, the paper furthers and enhances the theory of wave aberrations.

Appendix A: Sphere Function Coefficients

The coefficients for the sphere function are given in Table 17.

Appendix B: Aspheric Contributions

In this appendix we provide the change of wavefront deformation when the surface is aspheric. The difference in sag, $\Delta\{\text{Sag}\}$, between the sphere of vertex radius r and the aspheric surface is the aspheric cap,

$$\Delta\{\text{Sag}\} = A_4(X^2 + Y^2)^2 + A_6(X^2 + Y^2)^3, \quad (\text{B1})$$

where A_4 is the fourth-order coefficient of deformation and A_6 is the sixth-order coefficient of deformation. The fourth-order contributions to the wavefront deformation are given in Table 18. We wish to determine the sixth-order contributions from the aspheric cap that are contributed by the fourth-order coefficient A_4 . When the stop is at the surface, the sixth-order contributions are simple enough to derive with reasoning and the aid of real ray-tracing data and are

given in Table 19. To obtain the coefficients when the stop is shifted from the surface does requires elaborating the theory of stop shifting.

Now we wish to determine the change of sixth-order aberrations on stop shifting. By construction, the exit pupil coincides with the stop aperture. We start with the aperture stop located at the aspheric cap, and so the aberration function is given by

$$W_I^{+\text{cap}}(\vec{H}, \vec{\rho}) = W_{040}^{\text{cap}}(\vec{\rho} \cdot \vec{\rho})^2 + W_{240I}^{+\text{cap}}(\vec{H} \cdot \vec{H})(\vec{\rho} \cdot \vec{\rho})^2 + W_{311}^{+\text{cap}}(\vec{H} \cdot \vec{H})(\vec{H} \cdot \vec{\rho}) + W_{060I}^{+\text{cap}}(\vec{\rho} \cdot \vec{\rho})^3 + W_{151I}^{+\text{cap}}(\vec{H} \cdot \vec{\rho}) \cdot (\vec{\rho} \cdot \vec{\rho})^2, \quad (\text{B2})$$

where we have included the distortion term to account for the fact that the reference sphere is centered at the intersection of the chief ray with the Gaussian image plane. According to Eq. (32) the change in wavefront deformation on free-space propagation is

$$\Delta_Z W(\vec{H}, \vec{\rho}) = \frac{1}{2} \frac{\bar{y}}{y} \frac{1}{\Psi} \nabla_\rho W(\vec{H}, \vec{\rho}) \cdot \nabla_\rho W(\vec{H}, \vec{\rho}), \quad (\text{B3})$$

where \bar{y} is the new chief ray height and y is the marginal ray height at the old exit pupil aperture. The change of aperture vector from the old exit pupil to the new exit pupil produces a change of wavefront given by Eq. (34), or

$$\Delta W(\vec{H}, \vec{\rho}) = -\frac{1}{\Psi} \nabla_\rho W(\vec{H}, \vec{\rho}) \cdot \nabla_H \bar{W}(\vec{H}, \vec{\rho}). \quad (\text{B4})$$

As in the old exit pupil there is no error in defining a given ray, $\Delta\Omega = 0$,

$$\Delta W(\vec{H}, \vec{\rho}) = -\frac{\bar{y}}{y} \frac{1}{\Psi} \nabla_\rho W(\vec{H}, \vec{\rho}) \cdot \nabla_\rho W(\vec{H}, \vec{\rho}), \quad (\text{B5})$$

and the wavefront change on propagation and coordinate distortion between the old and new pupil is

Table 16. Sixth-Order Aberration Coefficients of the Triplet Lens in Waves at 587.6 nm

Sixth-Order Aberration Coefficients				
W_{040}	W_{131}	W_{222}	W_{220}	W_{311}
3.095E-013	4.842E-013	7.749E-014	-1.033E-013	1.2695E-012
W_{240}	W_{331}	W_{422}	W_{420}	W_{511}
4.3519E-012	-1.3257E-013	4.2807E-014	3.4504E-014	8.6500E-013
W_{060}	W_{151}	W_{242}	W_{333}	
1.011E-013	7.878E-014	-1.176E-012	-8.605E-014	
Fifth-Order Transverse Aberration Coefficients (mm)				
B	F	C	Pi	E
-6.71E-15	-2.522E-015	-3.537E-016	1.414E-015	-6.209E-015
B5	F1	F2	M1	M2
-3.5428E-15	-7.6113E-017	-5.187E-017	1.2030E-014	-9.6599E-014
N1	N2	N3	C5	Pi5
-2.536E-016	-4.7702E-016	-4.952E-017	-1.22E-016	-1.0157E-016
M3	E5			
1.252E-014	-4.851E-015			

$$\Delta W(\vec{H}, \vec{\rho}) = -\frac{1\bar{y}}{2y}\frac{1}{\Psi}\nabla_{\rho}W(\vec{H}, \vec{\rho}) \cdot \nabla_{\rho}W(\vec{H}, \vec{\rho}). \quad (\text{B6})$$

With $\Delta W_{\text{stopshift}}(\vec{H}, \vec{\rho})$ equal to the change of wavefront deformation on stop shifting from the center of curvature, we have that

$$\Delta W_{\text{stopshifting}}(\vec{H}, \vec{\rho}) = \left\{ W_{\text{cap}}(\vec{H}, \vec{\rho}) - \frac{1\bar{y}}{2y}\frac{1}{\Psi}\nabla_{\rho}W_{\text{cap}}(\vec{H}, \vec{\rho}) \cdot \nabla_{\rho}W_{\text{cap}}(\vec{H}, \vec{\rho}) \right\} \Big|_{\frac{\bar{y}}{y}\vec{H} + \vec{\rho}}, \quad (\text{B7})$$

where the terms inside the curly braces are evaluated at the shifted aperture vector $\vec{\rho} + (\bar{y}/y_{OP})\vec{H}$ and terms higher than sixth-order are neglected. We must account also for terms associated with the change of reference sphere; these terms are

$$\begin{aligned} \Delta \Xi(\vec{H}, \vec{\rho}) = & \frac{1}{2}W_{311}u'^2(\vec{H} \cdot \vec{H})(\vec{\rho} \cdot \vec{\rho})(\vec{H} \cdot \vec{\rho}) \\ & + W_{311}u'\bar{u}'(\vec{H} \cdot \vec{H})(\vec{H} \cdot \vec{\rho})^2 \\ & + \frac{1}{2}W_{311}u'\bar{u}'(\vec{H} \cdot \vec{H})^2(\vec{\rho} \cdot \vec{\rho}) \\ & + \frac{3}{2}W_{311}\bar{u}'^2(\vec{H} \cdot \vec{H})^2(\vec{H} \cdot \vec{\rho}) \\ & - \frac{1}{\Psi}[\nabla_{\rho}W_{311}(\vec{H} \cdot \vec{H})(\vec{H} \cdot \vec{\rho})] \cdot [\nabla_H\bar{W}(\vec{H}, \vec{\rho})]. \end{aligned} \quad (\text{B8})$$

Table 17. Coefficients of the Sphere Function Difference
 $n' \cdot \mathbf{S}'(\vec{H}, \vec{\rho}) - n \cdot \mathbf{S}(\vec{H}, \vec{\rho})$

Second-order	
$n'S'_{020} - nS_{020}$	$= -\frac{1}{2}\Psi\Delta\left\{\frac{u}{u'}\right\}$
$n'S'_{111} - nS_{111}$	$= -\Delta\{\Psi\} = 0$
$n'S'_{200} - nS_{200}$	$= -\frac{1}{2}\Psi\Delta\left\{\frac{\bar{u}}{\bar{u}'}\right\}$
Fourth order	
$n'S'_{040} - nS_{040}$	$= \frac{1}{8}\Psi\Delta\left\{\frac{u^3}{u'}\right\}$
$n'S'_{131} - nS_{131}$	$= \frac{1}{2}\Psi\Delta\{u^2\}$
$n'S'_{222} - nS_{222}$	$= \frac{1}{2}\Psi\Delta\{u\bar{u}\}$
$n'S'_{220} - nS_{220}$	$= \frac{1}{4}\Psi\Delta\{u\bar{u}\}$
$n'S'_{311} - nS_{311}$	$= \frac{1}{2}\Psi\Delta\{\bar{u}^2\}$
$n'S'_{400} - nS_{400}$	$= \frac{1}{8}\Psi\Delta\left\{\frac{\bar{u}^3}{\bar{u}'}\right\}$
Sixth order	
$n'S'_{060} - nS_{060}$	$= -\frac{1}{16}\Psi\Delta\left\{\frac{u^5}{u'}\right\}$
$n'S'_{151} - nS_{151}$	$= -\frac{3}{8}\Psi\Delta\{u^4\}$
$n'S'_{242} - nS_{242}$	$= -\frac{3}{4}\Psi\Delta\{u^3\bar{u}\}$
$n'S'_{333} - nS_{333}$	$= -\frac{1}{2}\Psi\Delta\{u^2\bar{u}^2\}$
$n'S'_{240} - nS_{240}$	$= -\frac{3}{16}\Psi\Delta\{u^3\bar{u}\}$
$n'S'_{331} - nS_{331}$	$= -\frac{12}{16}\Psi\Delta\{u^2\bar{u}^2\}$
$n'S'_{422} - nS_{422}$	$= -\frac{3}{4}\Psi\Delta\{u\bar{u}^3\}$
$n'S'_{420} - nS_{420}$	$= -\frac{3}{16}\Psi\Delta\{u\bar{u}^3\}$
$n'S'_{511} - nS_{511}$	$= -\frac{3}{8}\Psi\Delta\{\bar{u}^4\}$
$n'S'_{600} - nS_{600}$	$= -\frac{1}{16}\Psi\Delta\left\{\frac{\bar{u}^5}{\bar{u}'}\right\}$

Table 18. Fourth-Order Aberrations Contributed by an Aspheric Cap where A_4 is the Aspheric Coefficient

$W_{040}^{\text{cap}} = \Delta\{n\} \cdot A_4 \cdot y^4$	$\bar{W}_{040}^{\text{cap}} = \Delta\{n\} \cdot A_4 \cdot \bar{y}^4$
$W_{131}^{\text{cap}} = 4\Delta\{n\} \cdot A_4 \cdot y^3 \cdot \bar{y}$	$\bar{W}_{131}^{\text{cap}} = 4\Delta\{n\} \cdot A_4 \cdot \bar{y}^3 \cdot y$
$W_{222}^{\text{cap}} = 4\Delta\{n\} \cdot A_4 \cdot y^2 \cdot \bar{y}^2$	$\bar{W}_{222}^{\text{cap}} = 4\Delta\{n\} \cdot A_4 \cdot \bar{y}^2 \cdot y^2$
$W_{220}^{\text{cap}} = 2\Delta\{n\} \cdot A_4 \cdot y^2 \cdot \bar{y}^2$	$\bar{W}_{220}^{\text{cap}} = 2\Delta\{n\} \cdot A_4 \cdot \bar{y}^2 \cdot y^2$
$W_{311}^{\text{cap}} = 4\Delta\{n\} \cdot A_4 \cdot y \cdot \bar{y}^3$	$\bar{W}_{311}^{\text{cap}} = 4\Delta\{n\} \cdot A_4 \cdot \bar{y} \cdot y^3$
$W_{400}^{\text{cap}} = \Delta\{n\} \cdot A_4 \cdot \bar{y}^4$	$\bar{W}_{400}^{\text{cap}} = \Delta\{n\} \cdot A_4 \cdot y^4$

The results of this transformation are summarized in Table 20. The equations in Table 20 provide the sixth-order change of wavefront deformation as the stop is shifted from the aspheric cap defined by the coefficient A_4 . The extrinsic coefficients that arise between the aspheric cap and the base spherical surface are given by

$$W^{6E}(\vec{H}, \vec{\rho}) = -\frac{1}{\Psi}\nabla_{\rho}W_{\text{cap}}(\vec{H}, \vec{\rho}) \cdot \nabla_H\bar{W}_{\text{sphere}}(\vec{H}, \vec{\rho}), \quad (\text{B9})$$

$$\begin{aligned} \Delta\Pi(\vec{H}, \vec{\rho}) = & \frac{1}{2}W_{311}\Delta\{u^2\}(\vec{H} \cdot \vec{H})(\vec{\rho} \cdot \vec{\rho})(\vec{H} \cdot \vec{\rho}) \\ & + W_{311}\Delta\{u\bar{u}\}(\vec{H} \cdot \vec{H})(\vec{H} \cdot \vec{\rho})^2 \\ & + \frac{1}{2}W_{311}\Delta\{u\bar{u}\}(\vec{H} \cdot \vec{H})^2(\vec{\rho} \cdot \vec{\rho}) \\ & + \frac{3}{2}W_{311}\Delta\{\bar{u}^2\}(\vec{H} \cdot \vec{H})^2(\vec{H} \cdot \vec{\rho}). \end{aligned} \quad (\text{B10})$$

These terms are not included in Table 20 and should be added as intrinsic contributions from the aspheric surface.

The contributions to the coefficients from the sixth-order coefficient of deformation A_6 are given in Table 21; in this case there are no extrinsic contributions to the sixth-order level.

Appendix C: Spherical Contributions

In this Appendix we provide a derivation of the intrinsic coefficients on stop shifting for a spherical surface with the aperture vector at the exit pupil.

Table 19. Intrinsic Sixth-Order Aberrations Contributed by an Aspheric Cap^a

$W_{060}^{+\text{cap}} = -\frac{1}{2}\Delta\{n \cdot u^2\} \cdot A_4 \cdot y^4 + 2 \cdot W_{040}^{\text{cap}} \frac{y \cdot u}{r}$
$W_{151}^{+\text{cap}} = \frac{u}{yn'}\Psi \cdot W_{040}^{\text{cap}} + 3\frac{\Psi}{rn'}W_{040}^{\text{cap}} + \frac{8}{\Psi}W_{040}^{\text{cap}} \cdot W_{220P}$
$W_{242I}^{+\text{cap}} = 0$
$W_{333I}^{+\text{cap}} = 0$
$W_{240I}^{+\text{cap}} = \frac{1}{2nn'}\Psi^2 \cdot W_{040}^{\text{cap}} \frac{1}{y^2}$
$W_{331I}^{+\text{cap}} = 0$
$W_{422I}^{+\text{cap}} = 0$
$W_{420I}^{+\text{cap}} = 0$
$W_{511I}^{+\text{cap}} = 0$
$W_{600I}^{+\text{cap}} = 0$

^aThe stop is located at the cap, and the aperture vector is located at the exit pupil.

Table 20. Intrinsic Sixth-Order Aberrations Contributed by an Aspheric Cap as the Stop is Shifted^a

$$\begin{aligned}
 W_{060I}^+ &= W_{060I}^{+cap} - \frac{8}{\Psi} \frac{\bar{y}}{y} W_{040}^{cap} \cdot W_{040}^{cap} \\
 W_{151I}^+ &= W_{151I}^{+cap} + 6 \frac{\bar{y}}{y} W_{060I}^+ \\
 W_{242I}^+ &= 4 \left(\frac{\bar{y}}{y}\right) W_{151I}^{+cap} + 12 \left(\frac{\bar{y}}{y}\right)^2 W_{060I}^+ \\
 W_{333I}^+ &= 4 \left(\frac{\bar{y}}{y}\right)^2 W_{151I}^{+cap} + 8 \left(\frac{\bar{y}}{y}\right)^3 W_{060I}^+ \\
 W_{240I}^+ &= W_{240I}^{+cap} + \left(\frac{\bar{y}}{y}\right) W_{151I}^{+cap} + 3 \left(\frac{\bar{y}}{y}\right)^2 W_{060I}^+ \\
 W_{331I}^+ &= 4 \left(\frac{\bar{y}}{y}\right) W_{240I}^{+cap} + 6 \left(\frac{\bar{y}}{y}\right)^2 W_{151I}^{+cap} + 12 \left(\frac{\bar{y}}{y}\right)^3 W_{060I}^+ + \frac{1}{\Psi} W_{131}^{cap} \cdot W_{311}^{cap} - \frac{4}{\Psi} \left(\frac{\bar{y}}{y}\right) W_{040}^{cap} \cdot W_{311}^{cap} + \frac{1}{2} W_{311}^{cap} \cdot u \cdot u \\
 W_{422I}^+ &= 4 \left(\frac{\bar{y}}{y}\right)^2 W_{240I}^{+cap} + 8 \left(\frac{\bar{y}}{y}\right)^3 W_{151I}^{+cap} + 12 \left(\frac{\bar{y}}{y}\right)^4 W_{060I}^+ + \frac{2}{\Psi} W_{222}^{cap} \cdot W_{311}^{cap} - \frac{8}{\Psi} \left(\frac{\bar{y}}{y}\right)^2 W_{040}^{cap} \cdot W_{311}^{cap} + W_{311}^{cap} \cdot u \cdot \bar{u} \\
 W_{420I}^+ &= 2 \left(\frac{\bar{y}}{y}\right)^2 W_{240I}^{+cap} + 2 \left(\frac{\bar{y}}{y}\right)^3 W_{151I}^{+cap} + 3 \left(\frac{\bar{y}}{y}\right)^4 W_{060I}^+ + \frac{2}{\Psi} W_{220}^{cap} \cdot W_{311}^{cap} - \frac{4}{\Psi} \left(\frac{\bar{y}}{y}\right)^2 W_{040}^{cap} \cdot W_{311}^{cap} + \frac{1}{2} W_{311}^{cap} \cdot u \cdot \bar{u} \\
 W_{511I}^+ &= 4 \left(\frac{\bar{y}}{y}\right)^3 W_{240I}^{+cap} + 5 \left(\frac{\bar{y}}{y}\right)^4 W_{151I}^{+cap} + 6 \left(\frac{\bar{y}}{y}\right)^5 W_{060I}^+ + \frac{3}{\Psi} W_{311}^{cap} \cdot W_{311}^{cap} - \frac{12}{\Psi} \left(\frac{\bar{y}}{y}\right)^3 W_{040}^{cap} \cdot W_{311}^{cap} + \frac{3}{2} W_{311}^{cap} \cdot \bar{u} \cdot \bar{u} \\
 W_{600I}^+ &= \bar{W}_{060I}^+
 \end{aligned}$$

^aThe aperture vector is located at the exit pupil. The reference sphere is centered at the intersection of the chief ray with the Gaussian image plane.

Following the reasoning of Appendix B, the change of aberration function on stop shifting with the stop at the center of curvature is

$$\Delta W_{\text{stopshifting}}(\vec{H}, \vec{\rho}) = \left\{ W_{CC}^+(\vec{H}, \vec{\rho}) - \frac{1\bar{A}}{2A} \frac{1}{\Psi} \nabla_{\rho} W_{CC}^+(\vec{H}, \vec{\rho}) \cdot \nabla_{\rho} W_{CC}^+(\vec{H}, \vec{\rho}) \right\}_{(\bar{A}/A)\vec{H} + \vec{\rho}}, \quad (C1)$$

where $W_{CC}^+(\vec{H}, \vec{\rho})$ is

$$\begin{aligned}
 W_{CC}^+(\vec{H}, \vec{\rho}) &= W_{040}(\vec{\rho} \cdot \vec{\rho})^2 + W_{220}(\vec{H} \cdot \vec{H})(\vec{\rho} \cdot \vec{\rho}) \\
 &+ W_{240CC}^+(\vec{H} \cdot \vec{H})(\vec{\rho} \cdot \vec{\rho})^2 \\
 &+ W_{331CC}^+(\vec{H} \cdot \vec{H})(\vec{H} \cdot \vec{H})(\vec{\rho} \cdot \vec{\rho}) \\
 &+ W_{422CC}^+(\vec{H} \cdot \vec{H})(\vec{H} \cdot \vec{H})(\vec{H} \cdot \vec{H})(\vec{\rho} \cdot \vec{\rho}) \\
 &+ W_{420CC}^+(\vec{H} \cdot \vec{H})(\vec{H} \cdot \vec{H})^2(\vec{\rho} \cdot \vec{\rho}) \\
 &+ W_{060}^+(\vec{\rho} \cdot \vec{\rho})^3 + W_{151CC}^+(\vec{H} \cdot \vec{H})(\vec{\rho} \cdot \vec{\rho}) \cdot (\vec{\rho} \cdot \vec{\rho})^2 \\
 &+ W_{242CC}^+(\vec{H} \cdot \vec{H})(\vec{\rho} \cdot \vec{\rho})^2(\vec{\rho} \cdot \vec{\rho}) \\
 &+ W_{311}(\vec{H} \cdot \vec{H})(\vec{H} \cdot \vec{H})(\vec{H} \cdot \vec{H})(\vec{\rho} \cdot \vec{\rho}) \quad (C2)
 \end{aligned}$$

and where the effects of having the center of the reference sphere at the intersection of the chief ray with the Gaussian image plane are accounted for

Table 21. Sixth-Order Aberrations Contributed by an Aspheric Cap where A_6 is the Sixth-Order Aspheric Coefficient

$$\begin{aligned}
 W_{060I}^+ &= \Delta\{n\} \cdot A_6 \cdot y^6 \\
 W_{151I}^+ &= 6 \frac{\bar{y}}{y} W_{060I}^+ \\
 W_{242I}^+ &= 12 \left(\frac{\bar{y}}{y}\right)^2 W_{060I}^+ \\
 W_{333I}^+ &= 8 \left(\frac{\bar{y}}{y}\right)^3 W_{060I}^+ \\
 W_{240I}^+ &= 3 \left(\frac{\bar{y}}{y}\right)^2 W_{060I}^+ \\
 W_{331I}^+ &= 12 \left(\frac{\bar{y}}{y}\right)^3 W_{060I}^+ \\
 W_{422I}^+ &= 12 \left(\frac{\bar{y}}{y}\right)^4 W_{060I}^+ \\
 W_{420I}^+ &= 3 \left(\frac{\bar{y}}{y}\right)^4 W_{060I}^+ \\
 W_{511I}^+ &= 6 \left(\frac{\bar{y}}{y}\right)^5 W_{060I}^+ \\
 W_{600I}^+ &= \Delta\{n\} \cdot A_6 \cdot \bar{y}^6
 \end{aligned}$$

by adding the distortion term $W_{311}(\vec{H} \cdot \vec{H})(\vec{H} \cdot \vec{\rho})$. After the product of the gradients is obtained, stop shifting is performed by replacing $\vec{\rho}$ for the shifted vector $\vec{\rho} + (\bar{A}/A)\vec{H}$ and carrying out the expansion of terms and collecting similar terms.

The additional terms

$$\begin{aligned}
 \Delta \Xi(\vec{H}, \vec{\rho}) &= \frac{1}{2} W_{311} u^2 (\vec{H} \cdot \vec{H})(\vec{\rho} \cdot \vec{\rho})(\vec{H} \cdot \vec{\rho}) \\
 &+ W_{311} u \bar{u} (\vec{H} \cdot \vec{H})(\vec{H} \cdot \vec{\rho})^2 \\
 &+ \frac{1}{2} W_{311} u \bar{u} (\vec{H} \cdot \vec{H})^2 (\vec{\rho} \cdot \vec{\rho}) \\
 &+ \frac{3}{2} W_{311} \bar{u}^2 (\vec{H} \cdot \vec{H})^2 (\vec{H} \cdot \vec{\rho}) \\
 &- \frac{1}{\Psi} [\nabla_{\rho} W_{311}(\vec{H} \cdot \vec{H})(\vec{H} \cdot \vec{\rho})] \cdot [\nabla_H \bar{W}(\vec{H}, \vec{\rho})] \quad (C3)
 \end{aligned}$$

must also be added to account for the change of center of the reference sphere.

With the definitions in Table 22 the intrinsic coefficients on stop shifting are given in Table 23. The set of aberration coefficients in Tables 10 and 23 match each other to the 10^{-12} wave level. The differences are attributed to computation errors.

Note that the coefficients W_{331CC}^+ , W_{151CC}^+ , and W_{242CC}^+ in Table 22 differ from the corresponding ones in Table 9.

Appendix D: Derivation of Aberration Coefficients

In this Appendix we derive the aberration coefficients for spherical aberration, oblique spherical aberration, and field curvature.

1. Spherical Aberration W_{040} and W_{060}^-

With reference to Fig. 8, we have a spherical surface of radius of curvature r , a ray intersecting the surface at point P , intersecting the reference sphere at B' , intersecting the wavefront in object space at B and in image space at A' , and passing in image space by the point Q'' on the optical axis. The reference sphere in object space is centered at Q and in image

Table 22. Quantities used in the Calculation of the Intrinsic Aberration Coefficients with the Aperture Vector $\vec{\rho}$ at the Exit Pupil

$$\begin{aligned}
 W_{220P} &= -\frac{1}{4}\Psi^2 P \\
 W_{240CC}^+ &= +\frac{1}{16}\frac{A}{r}\Psi^2\Delta\left\{\frac{u}{n^2}\right\} + \frac{1}{8r}\Psi^2\Delta\left\{\frac{u^2}{n}\right\} \\
 &\quad + \frac{1}{4}\frac{u}{r}\Psi^2 W_{220P} + \frac{u}{r}W_{220P} - \frac{1}{4r}\Psi^2\Delta\left\{\frac{u}{n}\right\} \\
 W_{420CC}^+ &= \frac{3}{16}\frac{A}{r^3}\Psi^4\Delta\left\{\frac{1}{n}\right\} + \frac{1}{A^2}(W_{420CC}^+ = 0 \text{ for } A = 0) \\
 W_{331CC}^+ &= -2W_{220P} \cdot u' \bar{u}'_{CC} \\
 W_{422CC}^+ &= -W_{220P} \cdot \bar{u}'_{CC} \\
 W_{151CC}^+ &= -4W_{040} \cdot u' \bar{u}'_{CC} \\
 W_{242CC}^+ &= -2W_{040} \cdot \bar{u}'_{CC} \\
 \bar{u}'_{CC} &= \bar{u}' - \frac{A}{\Psi} u' \\
 P_{060} &= W_{040} \left[\frac{1}{2} \frac{v^2}{r^2} - \frac{1}{2} A \left(\frac{u'}{n'} + \frac{u}{n} \right) + 2 \frac{v}{r} u' \right] \\
 &\quad + \frac{8}{A^2} W_{040} W_{040} - \frac{A}{\Psi} W_{040} W_{040} \\
 P_{151} &= W_{151CC}^+ \\
 P_{240} &= W_{240CC}^+ - \frac{8}{\Psi} \frac{A}{A} W_{040} W_{220P} \\
 P_{331} &= W_{331CC}^+ - \frac{4}{\Psi} \frac{A}{A} W_{040} W_{331} \\
 P_{242} &= W_{242CC}^+ \\
 P_{420} &= W_{420CC}^+ - \frac{2}{\Psi} \frac{A}{A} W_{220P} W_{220P} - \frac{2}{\Psi} W_{220P} W_{311} \\
 P_{511} &= -\frac{2}{\Psi} \frac{A}{A} W_{220P} W_{311} \\
 C_{331} &= \frac{1}{\Psi} \bar{W}_{311} W_{311} + \frac{1}{2} W_{311} u u \\
 C_{422} &= \frac{2}{\Psi} \bar{W}_{222} W_{311} + W_{311} u \bar{u} \\
 C_{420} &= \frac{2}{\Psi} \bar{W}_{220} W_{311} + \frac{1}{2} W_{311} u \bar{u} \\
 C_{511} &= \frac{3}{\Psi} \bar{W}_{131} W_{311} + \frac{3}{2} W_{311} \bar{u} \bar{u}
 \end{aligned}$$

space is centered at Q' . After refraction the wavefront deformation is given by

$$W = n'[PB'] - n'[PA'] = n'[PB'] - n[PB], \quad (D1)$$

where $[PB'] = [OQ'] - [PQ']$ and $[PB] = [OQ] - [PQ]$. Since we are not using the actual point Q'' , the expression for $[PB']$ is not exact, and it leads to a tenth-order error in calculating W . Let the radius of the reference sphere in object and image space be $[OQ] = s$ and $[OQ'] = s'$, respectively, and the sag Z of the spherical surface to sixth-order be

$$Z = \frac{h^2}{2r} + \frac{h^4}{8r^3} + \frac{h^6}{16r^5}, \quad (D2)$$

where h is the height of the ray intersection with the spherical surface. The square of segment $[PQ]$ is given to sixth order by

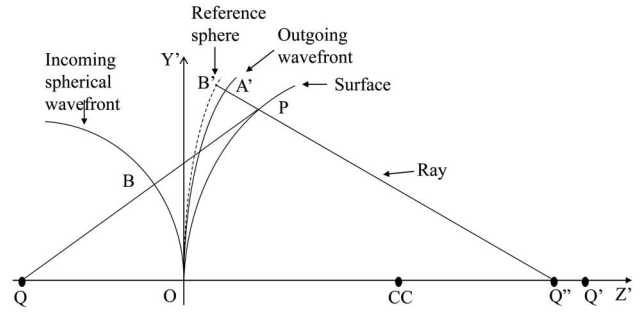


Fig. 8. Construction for deriving the wavefront deformation.

$$\begin{aligned}
 [PQ]^2 &= (s - Z)^2 + h^2 = s^2 - 2sZ + Z^2 + h^2 \\
 &= s^2 \left\{ 1 + \frac{h^2 - 2s \left[\frac{h^2}{2r} + \frac{h^4}{8r^3} + \frac{h^6}{16r^5} \right] + \left[\frac{h^4}{4r^2} + \frac{h^6}{8r^4} \right]}{s^2} \right\} \\
 &= s^2 \left\{ 1 + \frac{h^2}{s^2} \left[1 - \frac{s}{r} \right] + \frac{h^4}{4r^2 s^2} \left[1 - \frac{s}{r} \right] \right. \\
 &\quad \left. + \frac{h^6}{8r^4 s^2} \left[1 - \frac{s}{r} \right] \right\}, \quad (D3)
 \end{aligned}$$

and then the segment $[PB]$ is given to sixth order by

$$\begin{aligned}
 [PB] &= [OQ] - [PQ] \\
 &= -\frac{h^2}{2} \left[\frac{1}{s} - \frac{1}{r} \right] - \frac{h^4}{8r^2} \left[\frac{1}{s} - \frac{1}{r} \right] - \frac{h^6}{16r^4} \left[\frac{1}{s} - \frac{1}{r} \right] \\
 &\quad + \frac{h^4}{8s} \left[\frac{1}{s} - \frac{1}{r} \right]^2 + \frac{h^6}{16r^2 s} \left[\frac{1}{s} - \frac{1}{r} \right]^2 + \frac{h^6}{16s^2} \left[\frac{1}{s} - \frac{1}{r} \right]^3. \quad (D4)
 \end{aligned}$$

To third-order of approximation the ray intersection height h and the paraxial marginal ray height y are related by

$$h = y \left(1 + \frac{u}{2r} y \right), \quad (D5)$$

and so the segment $[PB]$ can be approximated to sixth order as

Table 23. Intrinsic Aberration Coefficients for a Spherical Surface with the Aperture Vector $\vec{\rho}$ at the Exit Pupil^a

$$\begin{aligned}
 W_{060I}^+ &= P_{060} \\
 W_{151I}^+ &= 6 \frac{A}{A} P_{060} + P_{151} \\
 W_{242I}^+ &= 12 \left(\frac{A}{A} \right)^2 P_{060} + 4 \left(\frac{A}{A} \right) P_{151} + P_{242} \\
 W_{333I}^+ &= 8 \left(\frac{A}{A} \right)^3 P_{060} + 4 \left(\frac{A}{A} \right)^2 P_{151} + 2 \left(\frac{A}{A} \right) P_{242} \\
 W_{240I}^+ &= 3 \left(\frac{A}{A} \right)^2 P_{060} + \left(\frac{A}{A} \right) P_{151} + P_{240} \\
 W_{331I}^+ &= 12 \left(\frac{A}{A} \right)^3 P_{060} + 6 \left(\frac{A}{A} \right)^2 P_{151} + 4 \left(\frac{A}{A} \right) P_{240} + 2 \left(\frac{A}{A} \right) P_{242} + P_{331} + C_{331} \\
 W_{422I}^+ &= 12 \left(\frac{A}{A} \right)^4 P_{060} + 8 \left(\frac{A}{A} \right)^3 P_{151} + 4 \left(\frac{A}{A} \right)^2 P_{240} + 5 \left(\frac{A}{A} \right)^2 P_{242} + 2 \left(\frac{A}{A} \right) P_{331} + P_{422} + C_{422} \\
 W_{420I}^+ &= 3 \left(\frac{A}{A} \right)^4 P_{060} + 2 \left(\frac{A}{A} \right)^3 P_{151} + 2 \left(\frac{A}{A} \right)^2 P_{240} + \left(\frac{A}{A} \right)^2 P_{242} + \left(\frac{A}{A} \right) P_{331} + P_{420} + C_{420} \\
 W_{511I}^+ &= 6 \left(\frac{A}{A} \right)^5 P_{060} + 5 \left(\frac{A}{A} \right)^4 P_{151} + 4 \left(\frac{A}{A} \right)^3 P_{240} + 4 \left(\frac{A}{A} \right)^3 P_{242} + 3 \left(\frac{A}{A} \right)^2 P_{331} + 2 \left(\frac{A}{A} \right) P_{422} + 2 \left(\frac{A}{A} \right) P_{420} + P_{511} + C_{511} \\
 W_{600I}^+ &= W_{060I}^+
 \end{aligned}$$

^aThe reference sphere is centered at the intersection of the chief ray with the Gaussian image plane.

$$\begin{aligned}
[PB] &= [OQ] - [PQ] \\
&= -\frac{y^2}{2} \left(1 + \frac{u}{2r}y\right)^2 \left[\frac{1}{s} - \frac{1}{r}\right] \\
&\quad - \frac{y^4}{8r^2} \left(1 + \frac{u}{2r}y\right)^4 \left[\frac{1}{s} - \frac{1}{r}\right] - \frac{y^6}{16r^4} \left[\frac{1}{s} - \frac{1}{r}\right] \\
&\quad + \frac{y^4}{8s} \left(1 + \frac{u}{2r}y\right)^4 \left[\frac{1}{s} - \frac{1}{r}\right]^2 + \frac{y^6}{16r^2s} \left[\frac{1}{s} - \frac{1}{r}\right]^2 \\
&\quad + \frac{y^6}{16s^2} \left[\frac{1}{s} - \frac{1}{r}\right]^3, \tag{D6}
\end{aligned}$$

and similarly for $[PB']$

$$\begin{aligned}
[PB'] &= [OQ'] - [PQ'] \\
&= -\frac{y^2}{2} \left(1 + \frac{u}{2r}y\right)^2 \left[\frac{1}{s'} - \frac{1}{r}\right] \\
&\quad - \frac{y^4}{8r^2} \left(1 + \frac{u}{2r}y\right)^4 \left[\frac{1}{s'} - \frac{1}{r}\right] - \frac{y^6}{16r^4} \left[\frac{1}{s'} - \frac{1}{r}\right] \\
&\quad + \frac{y^4}{8s'} \left(1 + \frac{u}{2r}y\right)^4 \left[\frac{1}{s'} - \frac{1}{r}\right]^2 + \frac{y^6}{16r^2s'} \left[\frac{1}{s'} - \frac{1}{r}\right]^2 \\
&\quad + \frac{y^6}{16s'^2} \left[\frac{1}{s'} - \frac{1}{r}\right]^3. \tag{D7}
\end{aligned}$$

Then we can write

$$\begin{aligned}
W &= n'[PB'] - n[PB] \\
&= -\frac{y^2}{2} \left(1 + \frac{u}{2r}y\right)^2 \left\{ n' \left[\frac{1}{s'} - \frac{1}{r}\right] - n \left[\frac{1}{s} - \frac{1}{r}\right] \right\} \\
&\quad - \frac{y^4}{8r^2} \left(1 + \frac{u}{2r}y\right)^4 \left\{ n' \left[\frac{1}{s'} - \frac{1}{r}\right] - n \left[\frac{1}{s} - \frac{1}{r}\right] \right\} \\
&\quad + \frac{y^4}{8} \left(1 + \frac{u}{2r}y\right)^4 \left\{ \frac{n'}{s'} \left[\frac{1}{s'} - \frac{1}{r}\right]^2 - \frac{n}{s} \left[\frac{1}{s} - \frac{1}{r}\right]^2 \right\} \\
&\quad - \frac{y^6}{16r^4} \left\{ n' \left[\frac{1}{s'} - \frac{1}{r}\right] - n \left[\frac{1}{s} - \frac{1}{r}\right] \right\} \\
&\quad + \frac{y^6}{16r^2} \left\{ \frac{n'}{s'} \left[\frac{1}{s'} - \frac{1}{r}\right]^2 - \frac{n}{s} \left[\frac{1}{s} - \frac{1}{r}\right]^2 \right\} \\
&\quad + \frac{y^6}{16} \left\{ \frac{n'}{s'^2} \left[\frac{1}{s'} - \frac{1}{r}\right]^3 - \frac{n}{s^2} \left[\frac{1}{s} - \frac{1}{r}\right]^3 \right\}. \tag{D8}
\end{aligned}$$

With $u = -y/s$, $u' = -y/s'$, $A = ni = -(y/s - y/r)$, and $\Delta\{A\} = 0$ the wavefront change W to sixth order is

$$\begin{aligned}
W &= -\frac{1}{8}A^2y\Delta\left\{\frac{u}{n}\right\} - \frac{1}{8}A^2y\Delta\left\{\frac{u}{n}\right\} \\
&\quad \times \left[\frac{y^2}{2r^2} - \frac{1}{2}A\left(\frac{u'}{n'} + \frac{u}{n}\right) + 2\frac{y}{r}u \right]. \tag{D9}
\end{aligned}$$

Thus we can write

$$W_{040} = -\frac{1}{8}A^2y\Delta\left\{\frac{u}{n}\right\}, \tag{D10}$$

$$W_{060}^- = W_{040} \left[\frac{y^2}{2r^2} - \frac{1}{2}A\left(\frac{u'}{n'} + \frac{u}{n}\right) + 2\frac{y}{r}u \right]. \tag{D11}$$

2. Petzval Field Curvature W_{220P} and Oblique Spherical Aberration W_{240CC}^-

Let us locate the aperture stop at the center of curvature of the spherical surface. With \bar{y}_0 being the object height, the inverse of the distance S along the chief ray from the off-axis object point to the surface is

$$\begin{aligned}
\frac{1}{-S} &= \frac{1}{-r + \sqrt{(r-s)^2 + \bar{y}_0^2}} = \frac{1}{-r + (r-s)\sqrt{1 + \frac{\bar{y}_0^2}{(r-s)^2}}} \\
&\cong \frac{1}{-r + (r-s)\left(1 + \frac{1}{2}\frac{\bar{y}_0^2}{(r-s)^2}\right)} = \frac{1}{-s\left(1 - \frac{1}{2}\frac{\bar{y}_0^2}{(r-s)s}\right)} \\
&= -\frac{1}{s}\left(1 + \frac{1}{2}\frac{\bar{y}_0^2}{(r-s)s}\right) = -\frac{1}{s}\left(1 + \frac{1}{2}\frac{\bar{y}_0^2}{\left(\frac{1}{s} - \frac{1}{r}\right)rs^2}\right) \\
&= -\frac{1}{s}\left(1 + \frac{u\bar{y}_0^2}{2irs}\right) = -\frac{1}{s} - \frac{u}{y^2} \frac{1}{2n^2ri} \Psi^2, \tag{D12}
\end{aligned}$$

and similarly for the inverse of the distance S' along the chief ray from the surface to the Gaussian image point,

$$\frac{1}{-S'} \cong -\frac{1}{s'} - \frac{u'}{y'^2} \frac{1}{2n'^2ri'}. \tag{D13}$$

Table 24. Constructional Data (mm) of the Triplet Lens^a

Surface Object	Radius	Thickness 10,000	Glass	A_4	A_6
1	255.635318	56.8473	BK7	-5.051563e-07	-3.2061469e-11
2	62.646002	23.6149		3.5999265e-007	9.4325832e-010
3	74.494599	15.7912	BK7	-1.0708598e-6	1.151724e-010
4	-58.717274	89.4891			
5	-42.87839	5	BK7	4.4688245e-007	-3.256491e-010
6	-203.330401	4.2124			
7		-65.250745			
Stop Image		65.249628			

^aThe exit pupil diameter is 14 mm, and the field angle is 15°; $\lambda = 587.6$ nm.

By inserting Eqs. (D12) and (D13) into the quadratic term y^2 of Eq. (D8), using $\Delta\{A\} = 0$, and retaining up to sixth-order terms, we obtain

$$\begin{aligned} W &= -\frac{y^2}{2} \left(1 + \frac{u}{2r}y\right)^2 \left\{ n' \left[\frac{1}{S'} - \frac{1}{r} \right] - n \left[\frac{1}{S} - \frac{1}{r} \right] \right\} \\ &= \left(1 + \frac{u}{2r}y\right)^2 \left\{ n'u' \left(-\frac{1}{4n'^2ri'} \right) - nu \left(-\frac{1}{4n^2ri} \right) \right\} \\ &= \left(1 + \frac{u}{2r}y\right)^2 \left\{ -\frac{1}{4Ar} \Psi^2 (u' - u) \right\} \\ &= \left(1 + \frac{u}{2r}y\right)^2 \left\{ -\frac{1}{4} \frac{\Psi^2}{r} \Delta \left\{ \frac{1}{n} \right\} \right\} \\ &= W_{220P} + u \frac{y}{r} W_{220P} + O^{(8)}. \end{aligned} \quad (D14)$$

By inserting Eqs. (D12) and (D13) into the first quartic term y^4 of Eq. (D8), using $\Delta\{A\} = 0$, and retaining up to sixth-order terms, we obtain

$$\begin{aligned} W &= -\frac{y^4}{8r^2} \left(1 + \frac{u}{2r}y\right)^4 \left\{ n' \left[\frac{1}{S'} - \frac{1}{r} \right] - n \left[\frac{1}{S} - \frac{1}{r} \right] \right\} \\ &= \frac{y^2}{4r^2} \left(1 + \frac{u}{2r}y\right)^4 \left\{ n'u' \left(-\frac{1}{4n'^2ri'} \right) - nu \left(-\frac{1}{4n^2ri} \right) \right\} \\ &= \frac{y^2}{4r^2} \left(1 + \frac{u}{2r}y\right)^4 \left\{ -\frac{1}{4} \frac{\Psi^2}{r} \Delta \left\{ \frac{1}{n} \right\} \right\} \\ &= \frac{y^2}{4r^2} W_{220P} + O^{(8)}. \end{aligned} \quad (D15)$$

By inserting Eqs. (D12) and (D13) into the second quartic term y^4 of Eq. (D8), using $\Delta\{A\} = 0$, and retaining up to sixth-order terms, we obtain

Thus for oblique spherical aberration W_{240CC}^- we have the terms

$$\frac{A}{16} \frac{\Psi^2}{r} \Delta \left(\frac{u}{n^2} \right) + \frac{1}{8} \frac{\Psi^2}{r} \Delta \left(\frac{u^2}{n} \right) + u \frac{y}{r} W_{220P} + \frac{y^2}{4r^2} W_{220P}. \quad (D17)$$

One effect that has not been accounted for is that for off-axis points the beam at the surface changes size by Δy to maintain the same size at the entrance pupil. The change in beam size is

$$\Delta y = -u' \Delta S' \frac{r}{s' - r} = \frac{1}{2} \frac{u' \Psi^2}{r A^2}, \quad (D18)$$

where

$$\Delta S' = \frac{1}{2} \frac{\Psi^2}{nu'Ar}. \quad (D19)$$

By replacing y with $y + \Delta y$ in the coefficient for spherical aberration and retaining the sixth-order term for oblique spherical aberration we find it to be $\frac{2u'\Psi^2}{ryA^2} W_{040} = -\frac{u'\Psi^2}{4r} \Delta \left(\frac{u}{n} \right)$. Thus the complete coefficient for oblique spherical aberration W_{240CC}^- becomes

$$\begin{aligned} W_{240CC}^- &= \frac{A}{16} \frac{\Psi^2}{r} \Delta \left(\frac{u}{n^2} \right) + \frac{1}{8} \frac{\Psi^2}{r} \Delta \left(\frac{u^2}{n} \right) + u \frac{y}{r} W_{220P} \\ &\quad + \frac{y^2}{4r^2} W_{220P} - \frac{u'\Psi^2}{4r} \Delta \left(\frac{u}{n} \right). \end{aligned} \quad (D21)$$

$$\begin{aligned} W &= \frac{y^4}{8} \left\{ \frac{n'}{S'} \left[\frac{1}{S'} - \frac{1}{r} \right]^2 - \frac{n}{S} \left[\frac{1}{S} - \frac{1}{r} \right]^2 \right\} = \frac{y^4}{8} \left\{ \frac{n'}{S'} \left[\frac{1}{s'} - \frac{1}{r} + \frac{u'1}{y^2 2n'^2 ri'} \right]^2 - \frac{n}{S} \left[\frac{1}{s} - \frac{1}{r} + \frac{u1}{y^2 2n^2 ri} \right]^2 \right\} \\ &= \frac{y^4}{8} \left\{ \frac{1}{n'S'} \left[n' \left(\frac{1}{s'} - \frac{1}{r} \right) + \frac{n'u'1}{y^2 2n'^2 ri'} \right]^2 - \frac{1}{nS} \left[n \left(\frac{1}{s} - \frac{1}{r} \right) + \frac{nu1}{y^2 2n^2 ri} \right]^2 \right\} = \frac{y^2}{8} \left\{ \frac{1}{n'S'} \left[-A' + \frac{u'1\Psi^2}{y 2rA'} \right]^2 \right. \\ &\quad \left. - \frac{1}{nS} \left[-A + \frac{u1\Psi^2}{y 2rA} \right]^2 \right\} = \frac{y^2 A^2}{8} \left\{ \frac{1}{n'S'} \left[-1 + \frac{u'1\Psi^2}{y 2rA'^2} \right]^2 - \frac{1}{nS} \left[-1 + \frac{u1\Psi^2}{y 2rA^2} \right]^2 \right\} \\ &= \frac{y^2 A^2}{8} \left\{ \frac{1}{n'S'} \left[1 - \frac{u'\Psi^2}{y r A'^2} \right] - \frac{1}{nS} \left[1 - \frac{u\Psi^2}{y r A^2} \right] \right\} + O^{(8)} = \frac{y^2 A^2}{8} \left\{ \frac{1}{n'} \left[\frac{1}{s'} + \frac{u'1}{y^2 2n'^2 ri'} \right] \left[1 - \frac{u'\Psi^2}{y r A'^2} \right] \right. \\ &\quad \left. - \frac{1}{n} \left[\frac{1}{s} + \frac{u1}{y^2 2n^2 ri} \right] \left[1 - \frac{u\Psi^2}{y r A^2} \right] \right\} + O^{(8)} = \frac{y A^2}{8} \left\{ \frac{u'}{n'} \left[-1 + \frac{1}{2yn'^2 ri'} \right] \left[1 - \frac{u'\Psi^2}{y r A'^2} \right] - \frac{u}{n} \left[-1 + \frac{1}{2yn^2 ri} \right] \left[1 - \frac{u\Psi^2}{y r A^2} \right] \right\} + O^{(8)} \\ &= \frac{y A^2}{8} \left\{ \frac{u'}{n'} \left[-1 + \frac{1}{2yn'^2 ri'} + \frac{u'\Psi^2}{y r A'^2} \right] - \frac{u}{n} \left[-1 + \frac{1}{2yn^2 ri} + \frac{u\Psi^2}{y r A^2} \right] \right\} + O^{(8)} = \frac{y A^2}{8} \left\{ -\left(\frac{u'}{n'} - \frac{u}{n} \right) + \frac{1}{2yrA'} \frac{\Psi^2}{n'^2} \left(\frac{u'}{n'^2} - \frac{u}{n^2} \right) \right. \\ &\quad \left. + \frac{1}{yrA^2} \left(\frac{u'^2}{n'^2} - \frac{u^2}{n^2} \right) \right\} + O^{(8)} = \frac{y A^2}{8} \left\{ -\Delta \left(\frac{u}{n} \right) + \frac{1}{2yrA'} \Delta \left(\frac{u}{n^2} \right) + \frac{1}{yrA^2} \Delta \left(\frac{u^2}{n} \right) \right\} + O^{(8)} \\ &= -\frac{A^2}{8} y \Delta \left(\frac{u}{n} \right) + \frac{A}{16} \frac{\Psi^2}{r} \Delta \left(\frac{u}{n^2} \right) + \frac{1}{8} \frac{\Psi^2}{r} \Delta \left(\frac{u^2}{n} \right) + O^{(8)}. \end{aligned} \quad (D16)$$

3. Petzval Field Curvature W_{220P} and W_{420CC}

Let us start with the relationship

$$\frac{1}{n'\rho'} - \frac{1}{n\rho} = \frac{n' - n}{n'nr} + \Lambda, \quad (\text{D22})$$

where ρ is the distance from the object to the center of curvature of the spherical surface, ρ' is the distance from the center of curvature to the image point, and Λ is a residual term when ρ and ρ' are not conjugate distances. Let us expand ρ as a function of the object height \bar{y}_0 ,

$$\frac{1}{\rho} = \frac{1}{\sqrt{\rho_0^2 + \bar{y}_0^2}} \cong \frac{1}{\rho_0} \left(1 - \frac{1\bar{y}_0^2}{2\rho_0^2} + \frac{3\bar{y}_0^4}{8\rho_0^4} \right), \quad (\text{D23})$$

and similarly for ρ' as

$$\frac{1}{\rho'} \cong \frac{1}{\rho'_0} \left(1 - \frac{1\bar{y}'_0{}^2}{2\rho'^2_0} + \frac{3\bar{y}'_0{}^4}{8\rho'^4_0} \right). \quad (\text{D24})$$

Along the optical axis $\bar{y}_0 = \bar{y}'_0 = 0$, and let us set

$$\frac{1}{n'\rho'_0} - \frac{1}{n\rho_0} = \frac{n' - n}{n'nr}. \quad (\text{D25})$$

Then substitution of Eqs. (D23) and (D24) into Eq. (D22) results in

$$\begin{aligned} \Lambda &= \frac{1}{n'\rho'_0} \left(1 - \frac{1\bar{y}'_0{}^2}{2\rho'^2_0} + \frac{3\bar{y}'_0{}^4}{8\rho'^4_0} \right) - \frac{1}{n\rho_0} \left(1 - \frac{1\bar{y}_0^2}{2\rho_0^2} + \frac{3\bar{y}_0^4}{8\rho_0^4} \right) \\ &\quad - \frac{n' - n}{n'nr} \\ &= -\frac{1}{2} \left(\frac{\bar{y}'_0{}^2}{n'\rho'^3_0} - \frac{\bar{y}_0^2}{n\rho_0^3} \right) + \frac{3}{8} \left(\frac{\bar{y}'_0{}^4}{n'\rho'^5_0} - \frac{\bar{y}_0^4}{n\rho_0^5} \right) \\ &= -\frac{1}{2} (u' - u) \frac{\Psi^2}{A^3 r^3} + \frac{3}{8} \left(\frac{1}{n'\rho'_0} - \frac{1}{n\rho_0} \right) \frac{\Psi^4}{A^4 r^4} \\ &= -\frac{1}{2} \frac{\Psi^2}{A^2 r^3} \Delta \left(\frac{1}{n} \right) + \frac{3}{8} \left(\frac{n' - n}{n'nr} \right) \frac{\Psi^4}{A^4 r^4}. \end{aligned} \quad (\text{D26})$$

Multiplying both members of Eq. (D26) by $A^2 r^2 / 2$ leads to

$$\frac{A^2 r^2 \Lambda}{2} = -\frac{1}{4} \frac{\Psi^2}{r} \Delta \left(\frac{1}{n} \right) + \frac{3}{16} \frac{\Psi^4}{A^2 r^3} \Delta \left(\frac{1}{n} \right). \quad (\text{D27})$$

The first term on the right-hand side of Eq. (D27) is the coefficient for Petzval field curvature W_{220P} , and

the second term is the coefficient for sixth-order field curvature W_{420CC} .

Appendix E

Data for the triplet lens are given in Table 24.

Macros

Computer macros for calculating the wave coefficients in codev, OSLO, and ZEMAX optical design software are available at <http://www.optics.arizona.edu/macros/wavecoefficients.zip>.

The grid figures illustrating the wavefront aberration shapes are a courtesy of Roland Shack, and the grid figures illustrating the effects of pupil aberrations are a courtesy of Lori Moore. We thank Ryan Irvin for carefully reading the manuscript and writing a codev macro to calculate the aberration coefficients. We thank Lambda Research for writing a macro file to calculate the coefficients in OSLO. The comments of Virendra Mahajan are much appreciated.

References

1. R. Shack, course OPTI 518, "Introduction to Aberrations," class notes, College of Optical Sciences, University of Arizona, 1995. The value of writing the aberration function in terms of the field and aperture vector is that further development in aberration theory is possible. See, for example, [2] and the contributions in this paper as examples.
2. K. Thompson, "Description of the third-order optical aberrations of near-circular pupil optical systems without symmetry," *J. Opt. Soc. Am.* **22**, 1389–1401 (2005).
3. K. Schwarzschild, "Untersuchungen zur geometrischen Optik I. Einleitung in die Fehlertheorie optischer Instrumente auf Grund des Eikonalbegriffs," *Abh. Königlichen Ges. Wiss. Göttingen Math. Phys. Kl.* **4**, 1–31 (1905).
4. H. H. Hopkins, *The Wave Theory of Aberrations* (Oxford Univ. Press, 1950).
5. C. G. Wynne, "Primary aberrations and conjugate change," *Proc. Phys. Soc. London Sect. B* **65**, 429–437 (1952).
6. J. Hoffman, "Induced aberrations in optical systems," Ph. D. dissertation (University of Arizona, 1993).
7. J. Sasian, "Interpretation of pupil aberrations in imaging systems," *Proc. SPIE* **634**, 634208 (2006).
8. J. Sasian, "Design of null lens correctors for the testing of astronomical optics," *Opt. Eng.* **27**, 1051–1056 (1988).
9. D. Shafer's triplet lens data can be found in [6].
10. M. P. Rimmer, "Optical aberration coefficients," M.S. thesis (University of Rochester, 1963).
11. H. A. Buchdahl, *Optical Aberration Coefficients* (Dover, 1968).
12. M. R. Teague, "Image formation in terms of the transport equation," *J. Opt. Soc. Am. A* **2**, 2019–2026 (1985).